Chapter 5

Tracking a Single Target under Measurement Origin Uncertainty in Wireless Sensor Networks

This chapter addresses the problem of tracking a single target under measurement origin uncertainty due to clutter and missed detections in wireless sensor networks. By using particles to represent the probability density function of the target state, this chapter develops the Particle filter (PF) and probabilistic data association filter (PDAF) hybrid tracking algorithm, name as PF-PDAF. The PF-PDAF algorithm extends the well-known PDAF to the general nonlinear system in an attempt to make use of the advantages of PDAF in effectively dealing with clutter and missed detections. To provide a theoretical lower bound on the tracking performance under measurement origin uncertainty, the posterior Cramer-Rao lower bound (PCRLB) that takes into consideration of clutter and missed detections is derived and computed in this chapter.

5.1 Introduction

In most practical single target tracking applications in wireless sensor networks, a sensing node may acquire more than one measurement. These measurements typically include the measurement generated by the target to be tracked (assuming this target is detected) and the measurements originated from clutter. Here, the term “clutter” refers to the undesired objects that may originate from the terrain, thermal noises, electromagnetic interference, and acoustic anomalies. Generally, the clutter originated measurements are random in number, location and intensity [27], [47]. Another complicating aspect is that, at some time steps, the target may be undetected by the sensor nodes. This is referred to as missed detections. Under measurement origin uncertainty due to clutter and missed detections, the tracking algorithm needs to first solve the so-called data association problem that distinguishes the target originated measurement from clutter originated measurements; and then it can incorporate the right measurement for the target state estimate [47], [132].

The aim of this chapter is to develop techniques and algorithms for tracking a single target under measurement origin uncertainty resulting from the aforementioned clutter and missed detections. Using the particles' representation of the probability density function of the target state, the traditional probabilistic data association filter (PDAF) is extended to handle the general nonlinear state space model, while the advantages of PDAF in solving the data association problem are kept. To provide the theoretical lower bound on the tracking performance under measurement origin uncertainty, the PCRLB that takes into account the clutter and missed detections is also derived and computed.

This chapter is structured as follows. In Section 5.2, the problem of tracking a single target under measurement origin uncertainty in a wireless sensor network is formulated. In Section 5.3, the hybrid PF-PDAF algorithm for tracking a single target under measurement origin uncertainty in wireless sensor networks is developed. In Section 5.4, the PCRLB that consider the clutter and missed detections is derived and computed. In Section 5.5, simulations are conducted on various synthetic tracking scenarios to assess the performance of PF-PDAF algorithm. Moreover, simulations are also carried out to compare the root square PCRLB values with RMSE values on the synthetic tracking scenarios. Finally, in Section 5.6 the conclusion remarks are provided.

5.2 Problem Formulation

This section formulates the problem of tracking a single target with clutter and missed detections in a wireless sensor network. It is assumed that over the full duration of a tracking task, the target moves in space spanned by a sensor node cluster which employs a leader node and a fix set of N_s sensing node (termed as active sensing nodes). The state space model for this setting can be written as follows:

$$\mathbf{x}_{k+1} = \mathbf{A}_k \mathbf{x}_k + \mathbf{v}_k \tag{5.1}$$

$$\mathbf{z}_{t,k}^{n} = \quad \mathbf{h}_k^n \left(\mathbf{x}_k, \ \mathbf{n}_k^n \right) \quad n = 1,..., N_s \tag{5.2}$$

Equation 5.1 is the system model, and this chapter adopts the nearly constant velocity (CV) model as in Chapter 4. In Equation 5.1, $\mathbf{x}_k$ is the target state at time step k which is given by $\mathbf{x}_k = \left[\ x, v_x \ , y, v_y \ \right]_k^T$, where x and y are the target positions in x- and y-coordinate respectively while v_x and v_y are the target velocities in x- and y-coordinate, respectively.

$\mathbf{x}_k$ is assumed to be unobserved with initial probability distribution $p(\mathbf{x}_0)$. $\mathbf{A}_k$ is the system transition matrix. $\mathbf{v}_k$ is the process noise vector and assumed to be Gaussian with zero mean and covariance matrix $\mathbf{Q}_k$, i.e. $\mathrm{v}_k \sim N(\mathbf{0}, \mathbf{Q}_k)$. $\mathbf{A}_k$ and $\mathbf{Q}_k$ for the CV model are already given in Chapter 4. In Equation 5.2, the superscript n refers to the n-th sensing node; the first subscript t refers to the t-th target (however, in this chapter there is only one target); and the second subscript k denotes the k-th time step. In other words, $\mathbf{z}_{t,k}^n$ denotes the target originated measurement acquired by the n-th sensing node at the k-th time step. $\mathbf{h}_k^n$ is the measurement function of the n-th sensing node at the k-th time step. As mentioned earlier in Chapter 4, the measurement model adopted throughout this thesis is nonlinear; hence $\mathbf{h}_k^n$ is a nonlinear function (repeated in Equation 5.3). $\mathbf{n}_k^n$ is the measurement noise at the n-th sensing node and it is assumed to be Gaussian with mean $\boldsymbol{\mu}_k^n$ and covariance matrix $\mathbf{R}_k^n$, i.e. $\mathbf{n}_k^n \sim N(\boldsymbol{\mu}_k^n, \mathbf{R}_k^n)$.

Under the measurement origin uncertainty, at a particular time step k, the n-th sensing node acquires a set of measurements which may include the measurement generated by the target as well as measurements originated from clutter. This set of measurements is designated as $\mathbf{Z}_k^n = \left(\mathbf{z}_{1,k}^n, ..., \mathbf{z}_{j,k}^n, ..., \mathbf{z}_{l_k^n,k}^n\right), \quad j = 1, ..., l_k^n$, where l_k^n is the total number of measurements acquired by the n-th sensing node at the k-th time step. In practice, these l_k^n measurements can all be clutter originated measurements, or there is one target originated measurement and $l_k^n - 1$ clutter originated measurements. At time step k, the concatenated measurement over all N_s sensing nodes that involve in the tracking task is denoted as $\mathbf{Z}_k = \left(\mathbf{Z}_k^1, ..., \mathbf{Z}_k^{N_s}\right)$. The time aggregated measurement from the initial time step to the k-th time step is denoted as $\mathbf{Z}_{0:k} = \left(\mathbf{Z}_0, ..., \mathbf{Z}_k\right)$.

The model of target originated measurement has already been defined in Equation 4.6 of Chapter 4. For convenience, the equation is re-written here

$$\left\| \mathbf{z}_{t,k}^n \right\| = \frac{S_k}{\left\| \boldsymbol{\rho}_k - \mathbf{r}_k^n \right\|^2} + \varepsilon_k^n \tag{5.3}$$

where S_k is the intensity of the acoustic signal generated by the target at the k-th time step, and $\varepsilon_k^n \sim N\left(0, \mathbf{R}_k^n\right)$ is the additive Gaussian noise with zero mean and covariance $\mathbf{R}_k^n$ at the n-th sensing node. $\boldsymbol{\rho}_k$ and $\mathbf{r}_k^n$ are the position coordinates of the target and the n-th sensing node, respectively.

The clutter originated measurements are assumed to be independent and uniformly distributed over the observation space V of a sensing node with the probability

$$p_{0,k}^n\left(\mathbf{z}_{j,k}^n\right) = p\left(\mathbf{z}_{j,k}^n \,\middle|\, \mathbf{z}_{j,k}^n \text{ is the clutter originated measurment}\right) = \frac{1}{V} \quad j \in \left(1,..., l_k^n\right) \tag{5.4}$$

It is assumed throughout this thesis that all sensing nodes have the same observation space V. This assumption coincides with the nature of a wireless sensor network: a large number of homogeneous sensing nodes with the identical transmission range, sensing modalities and initial energy are deployed around the observed phenomena (i.e. moving target) to provide unbiased and consistent information.

In target tracking, it is commonly assumed that the number of the clutter originated measurements in the observation space V of a sensing node follows a Poisson probability mass function (pmf) given by [27]

$$P_F\left(l_{C,k}^n\right) = \exp\left(-\lambda V\right) \frac{\left(\lambda V\right)^{l_{C,k}^n}}{l_{C,k}^n\,!} \tag{5.5}$$

where λ is the clutter rate which is defined as the number of clutter generated measurements per unit volume of the observation space. $l_{C,k}^n$ is the number of clutter originated measurements obtained at the n-th sensing node during the k-th time step.

The assumptions that have been made in Section 4.2 of Chapter 4 are retained throughout this chapter. Among these assumptions, we emphasize the independent assumptions made for the measurement noises and the process noise: the measurement noises and the process noise are uncorrelated; the measurement noises are not correlated at the same sensing node and amongst different sensing nodes. In addition, in this chapter we also make two more assumptions:

(1) The target can be either detected or undetected by a sensing node.

(2) At each time step, each sensing node can provide more than one measurement because of the presence of clutter. It is assumed that the measurements acquired at an individual

sensing node are already separated by some means of signal processing [21]. However, the sources or labels of these measurements are unavailable from the sensing nodes.

5.3 PF-PDAF for Tracking a Single Target under Measurement Origin Uncertainty in Wireless Sensor Networks

The hybrid PF-PDAF is a straightforward implementation of PDAF by using particles to represent the probability density function of the target state. Since the target might be undetected at the n-th sensing node, we denote the probability of the target being detected or the detection rate as P_d. For the sake of clarity and without losing the generality, it is assumed throughout this thesis that P_d is time invariant. It is also assumed that P_d takes the same value across all sensing nodes since we adopt the homogeneous sensing nodes with the same sensing modality and signal processing functionalities for target tracking in wireless sensor networks. With the detection rate P_d and the probability distribution of the number of the clutter originated measurements (Equation 5.5), the prior probability that there are l_k^n measurements at the k-th time step can be expressed as

$$\begin{aligned} P\left(l_k^n\right) &= \left(1-P_d\right)P_F\left(l_k^n\right) + P_d\, P_F\left(l_k^n - 1\right) \\ &= \left(1-P_d\right)\frac{\left(\lambda V\right)^{l_k^n}\exp\left(-\lambda V\right)}{l_k^n\,!} + P_d\,\frac{\left(\lambda V\right)^{l_k^n-1}\exp\left(-\lambda V\right)}{\left(l_k^n-1\right)!} \end{aligned} \tag{5.6}$$

In turn, the probability that one particular measurement is target originated is given by

$$\varepsilon\left(l_k^n\right) = \frac{P_d}{P\left(l_k^n\right)}\frac{\left(\lambda V\right)^{\left(l_k^n-1\right)}\exp\left(-\lambda V\right)}{\left(l_k^n-1\right)!} \tag{5.7}$$

At the k-th time step, for the n-th sensing node, the probability density function of the measurement likelihood given the target state $\mathbf{x}_k$ and the number of measurements l_k^n, $p\left(\mathbf{Z}_k^n \middle| \mathrm{x}_k, l_k^n\right)$ can be derived as follows

$$\begin{aligned} p\left(\mathbf{Z}_k^n \middle| \mathbf{x}_k, l_k^n\right) &= p\left(\mathbf{Z}_k^n \middle| l_k^n, \zeta_{0,k}^n, \mathbf{x}_k\right)P\left(\zeta_{0,k}^n \middle| l_k^n\right) + p\left(\mathbf{Z}_k^n \middle| l_k^n, \zeta_{j,k}^n, \mathbf{x}_k\right)P\left(\zeta_{j,k}^n \middle| l_k^n\right) \\ &= \left[1-\varepsilon\left(l_k^n\right)\right]p\left(\left\{\mathbf{z}_{j,k}^n\right\}_{j=1}^{l_k^n} \middle| \zeta_{0,k}^n, \mathbf{x}_k\right) + \sum_{j=1}^{l_k^n}\frac{\varepsilon\left(l_k^n\right)}{l_k^n}p\left(\left\{\mathbf{z}_{j,k}^n\right\}_{j=1}^{l_k^n} \middle| \zeta_{j,k}^n, \mathbf{x}_k\right) \end{aligned} \tag{5.8}$$

where $\zeta_{0,k}^{n}$ denotes the event of having all measurements obtained by the n-th sensing node at the k-th time step are clutter originated; and $P\left(\zeta_{0,k}^{n} \middle| l_k^n\right)$ is the prior probability of having event $\zeta_{0,k}^{n}$ given l_k^n measurements. $\zeta_{j,k}^{n}$, $j=1,...,l_k^n$ denotes the event of having one target originated measurement amongst l_k^n measurements obtained by the n-th sensing node at the k-th time step; and $P\left(\zeta_{j,k}^{n} \middle| l_k^n\right)$ is the prior probability of $\mathbf{z}_{j,k}^{n}$, $j=1,...,l_k^n$ being the target originated measurement. Substituting Equation 5.4 into 5.8, we obtain

$$p\left(\mathbf{Z}_k^n \middle| \mathbf{x}_k, l_k^n\right) = \frac{\left(1-\varepsilon\left(l_k^n\right)\right)}{V^{l_k^n}} + \frac{\varepsilon\left(l_k^n\right)}{V^{l_k^n-1} l_k} \times \sum_{j=1}^{l_k^n} p\left(\mathbf{z}_{j,k}^{n} \middle| \mathbf{x}_k\right) \tag{5.9}$$

where $p\left(\mathbf{z}_{j,k}^{n} \middle| \mathbf{x}_k\right)$ is the likelihood of the j-th measurement obtained at the n-th sensing node with respect to the target state $\mathbf{x}_k$ at the k-th time step and it is given by

$$p\left(\mathbf{z}_{j,k}^{n} \middle| \mathbf{x}_k\right) = \frac{1}{\sqrt{\left|2\pi \mathbf{R}_k^n\right|}} \exp\left[-\frac{1}{2}\left(\mathbf{z}_{j,k}^{n} - \hat{\mathbf{H}}_k^n \mathbf{x}_k\right)^T \left(\mathbf{R}_k^n\right)^{-1} \left(\mathbf{z}_{j,k}^{n} - \hat{\mathbf{H}}_k^n \mathbf{x}_k\right)\right] \tag{5.10}$$

where $\mathbf{R}_k^n$ is the covariance matrix of the measurement noise and $\hat{\mathbf{H}}_k^n$ is the Jacobian matrix of $\mathbf{h}_k^n$ and defined as follows

$$\hat{\mathbf{H}}_k^n = \left.\frac{d\,\mathbf{h}_k^n(\mathbf{x})}{d\,\mathbf{x}}\right|_{\mathbf{x}=\mathbf{m}_{k|k-1}} \tag{5.11}$$

where $\mathbf{m}_{k|k-1} = \mathbf{A}_k\, \mathbf{m}_{k-1|k-1}$ and $\mathbf{m}_{k-1|k-1}$ is the mean of target state estimate obtained at the previous time step, i.e. the $(k-1)$-th time step.

Supposing that at the $(k-1)$-th time step, the probability density function of the target state, i.e. $p\left(\mathbf{x}_{k-1} \middle| \mathbf{Z}_{0:k-1}\right)$ is already known and approximated by a set of N particles together with their weights $\left\{\mathbf{x}_{k-1,}^{i}, w_{k-1}^{i}\right\}_{i=1}^{N}$, the process of PF-PDAF to obtain $p\left(\mathbf{x}_k \middle| \mathbf{Z}_{0:k}\right)$ at the k-th is as follows. At the k-th time step, the N_s sensing nodes are activated to sense and then transmit their measurements to the cluster leader.

Correspondingly, the cluster leader will receive total N_s sets of measurements with each set contains $l_k^n, n = 1,...,N_s$ measurements. Upon receiving these measurements, the cluster leader executes PF-PDAF algorithm to update the target state estimate for the k-th time step. In this PF-PDAF, the new set of particles $\left\{ \mathbf{x}_k^i \right\}_{i=1}^N$ at the k-th time step is drawn from the transition prior $p\left(\mathbf{x}_k^i \middle| \mathbf{x}_{k-1}^i\right)$ (i.e. adopting transition prior as the proposal distribution).

Similar to the PF and EKPF tracking algorithms in Chapter 4, PF-PDAF algorithm mixes the measurements from different sensing nodes into a single likelihood function for multiple sensing nodes. The measurements independence assumption made in Section 5.2 allows for the factorization of this measurement likelihood over N_s sensing nodes:

$$p\left(\mathbf{Z}_k \middle| \mathbf{x}_k^i\right) = \prod_n^{N_s} p\left(\mathbf{Z}_k^n \middle| \mathbf{x}_k^i, l_k^n\right), \quad i = 1,...,N \tag{5.12}$$

Note that in Equation 5.12, $\mathbf{x}_k^i$ denotes the i-th particle. Combining Equations 5.6, 5.7 and 5.9~5.12, the new importance weight of i-th particle can be set as

$$\begin{aligned} w_k^i &= w_{k-1}^i \, p\left(\mathbf{Z}_k \middle| \mathbf{x}_k^i\right) \\ &= w_{k-1}^i \prod_n^{N_s} \left[\frac{\left(1-\varepsilon\left(l_k^n\right)\right)}{V^{l_k^n}} + \frac{\varepsilon\left(l_k^n\right)}{V^{l_k^n-1} l_k} \times \sum_{j=1}^{l_k^n} p\left(\mathbf{z}_{j,k}^n \middle| \mathbf{x}_k\right) \right] \end{aligned} \tag{5.13}$$

where $p\left(\mathbf{z}_{j,k}^n \middle| \mathbf{x}_k\right)$ is computed according to Equation 5.10. Consequently, a set of new particles $\left\{ \mathbf{x}_k^i, w_k^i \right\}_{i=1}^N$ are obtained to approximate the probability distribution density of target state $p\left(\mathbf{x}_k \middle| \mathbf{Z}_{0:k}\right)$ at the k-th time step. After the resampling step, $p(\mathbf{x}_k \,|\, \mathbf{Z}_{0:k})$ can be approximated as follows

$$\hat{p}(\mathbf{x}_k \,|\, \mathbf{Z}_{0:k}) = \frac{1}{N} \sum_{i=1}^N \delta\left(\mathbf{x}_k - \mathbf{x}_k^{i*}\right) \tag{5.14}$$

where δ is the Dirac function and $\mathbf{x}_k^{i*}$ is the particles obtained after the resampling step. The complete PF-PDAF tracking algorithm is listed below.

Algorithm 5.1 PF-PDAF Tracking Algorithm for Single Target Tracking under Measurement Origin Uncertainty in Wireless Sensor Networks

- Initialization: $k = 0$

  For $i = 1, 2, ..., N$ draw particle $\mathbf{x}_k^i$ from the prior $p(\mathbf{x}_0)$.

- For time steps $k = 1, 2, ...$

  - For $i = 1, 2, ..., N$, draw sample $\mathbf{x}_k^i \sim p(\mathbf{x}_k \mid \mathbf{x}_{k-1}^i)$.

  - For $i = 1, 2, ..., N$, evaluate the importance weights as per following steps

    . For $n = 1, 2, ... N_s$ sets of measurements from N_s sensing nodes, do

$$p(\mathbf{Z}_k^n \mid \mathbf{x}_k^i, l_k^n) = \frac{(1 - \varepsilon(l_k^n))}{V^{l_k^n}} + \frac{\varepsilon(l_k^n)}{V^{l_k^n - 1} l_k} \times \sum_{j=1}^{l_k^n} p(\mathbf{z}_{j,k}^n \mid \mathbf{x}_k^i)$$

where

$$\varepsilon(l_k^n) = \frac{P_d}{P(l_k^n)} \frac{(\lambda V)^{(l_k^n - 1)} \exp(-\lambda V)}{(l_k^n - 1)!}$$

$$P(l_k^n) = (1 - P_d) \frac{(\lambda V)^{l_k^n} \exp(-\lambda V)}{l_k^n!} + P_d \frac{(\lambda V)^{l_k^n - 1} \exp(-\lambda V)}{(l_k^n - 1)!}$$

$$p(\mathbf{z}_{j,k}^n \mid \mathbf{x}_k^i) = \frac{1}{\sqrt{|2\pi \mathbf{R}_k^n|}} \exp\left[-\frac{1}{2} (\mathbf{z}_{j,k}^n - \hat{\mathbf{H}}_k^n \mathbf{x}_k^i)^T (\mathbf{R}_k^n)^{-1} (\mathbf{z}_{j,k}^n - \hat{\mathbf{H}}_k^n \mathbf{x}_k^i) \right]$$

and

$$\hat{\mathbf{H}}_k^n = \left. \frac{d \mathbf{h}_k^n(\mathbf{x})}{d \mathbf{x}} \right|_{\mathbf{x} = \mathbf{m}_{k \mid k-1}}$$

    . Compute the importance weights of particles

$$w_k^i = w_{k-1}^i \prod_n^{N_s} \left[\frac{(1 - \varepsilon(l_k^n))}{V^{l_k^n}} + \frac{\varepsilon(l_k^n)}{V^{l_k^n - 1} l_k} \times \sum_{j=1}^{l_k^n} p(\mathbf{z}_{j,k}^n \mid \mathbf{x}_k^i) \right]$$

  - For $i = 1, 2, ..., N$, normalize the importance weights: $\tilde{w}_k^i = w_k^i \Big/ \sum_{j=1}^{N} w_k^j$

  - Multiply (suppress) particles $\mathbf{x}_k^i$ with high (low) importance weights $\tilde{w}_k^i$ to obtain

    N new particles $\mathbf{x}_k^{i*}$ that are approximately distributed according to $p(\mathbf{x}_k \mid \mathbf{Z}_{0:k})$.

  - For $i = 1, 2, ..., N$, reset the importance weights $w_k^i = \tilde{w}_k^i = N^{-1}$.

- Output: The output of the algorithm is a set of particles that can be used to approximate

the probability density function of target state, i.e. $\hat{p}(\mathbf{x}_k|\mathbf{Z}_{0:k}) = \frac{1}{N}\sum_{i=1}^{N}\delta\left(\mathbf{x}_k - \mathbf{x}_k^{i*}\right)$.

The above process is the general implementation of the PF-PDAF algorithm for tracking a single target under measurement origin uncertainty in a wireless sensor network. However, there still remains some design issues, for example, the measurement selection (gating) procedure and the proposal distribution design. These two issues are briefly discussed below.

Gating procedure aims to preclude the measurements that are far from the predicted measurement region and thus to reduce the computation load [27]. Physical justification is that such measurements are likely to be erroneous and would not contribute information about the target. Normally, gating is performed at each time step by defining an area of measurement space which is called gate. All measurements located in the gate are selected and used for the target state estimation while the measurements not in the gate are ignored. There are a number of gating schemes in the literature including centralized gating, model based gating, model probability weighted gating and two-stage model probability weighted gating [27], [133], [155]. However, the detailed discussion of the gating design is beyond the scope of this chapter. Instead of explicitly employing the above gating procedure, the PF-PDAF tracking algorithm developed in this chapter implements a simple and efficient sensing nodes selection scheme to achieve “soft” gating. The strategy adopted uses only the measurements from three sensing nodes that are closest to the predicted target position at each time step for the target state estimation. This immediately implies that the measurements from sensing nodes which are far from the predicted target position are precluded from the target state estimation. Apparently, the above method is also effective in precluding a considerable amount of clutter originated measurements, since we can infer from SNR considerations that more accurate measurements are made by nearby sensing nodes.

In the above PF-PDAF algorithm, the transition prior is taken as the proposal distribution. This choice of proposal distribution makes the algorithmic implementation straightforward. However, as discussed in Chapter 4, it may lead to inefficient algorithms since the particles cannot be moved to high measurement likelihood area in the state space. To design a better proposal distribution, at first it seems reasonable to resort to the approach similar to the one that adopted in EKPF that uses EKF to take into account the latest target generating measurement. However, under the measurement origin uncertainty

due to the clutter and missed detections, it is not a trivial task to pick up the target generating measurement in the prediction step before solving the data association problem in the update step. Therefore, it is fundamentally difficult to directly implement a hybrid EKF and PDAF tracking algorithm analogue to the EPKF development in Chapter 4.

One solution to the above problem is to adopt a mixture proposal distribution in which one portion of the new particles is generated from the transition prior while the reminder of the new particles are sampled from a mixture with each component of this mixture accounting for one measurement either generated by the target or generated by the clutter [48]. Evidently, such a solution will increase the implementation complexity and the computation burden. Moreover, in this mixture proposal distribution, some particles may be moved to the high likelihood area while other particles may move far away from the high likelihood area since they are propagated by incorporating the clutter generated measurements. Consequently, the overall performance of the PF-PDAF which adopts mixture proposal cannot justify the extra algorithmic complexity and computation burden it introduces. In Chapter 7, the above mixture proposal distribution is developed for multiple target tracking in a wireless sensor network and the simulation results do not show much improvement over the transition prior approach.

5.4 PCRLB Calculation under Measurement Origin Uncertainty

The PCRLB in Chapter 4 is calculated with the assumption of no clutter and missed detections. This section will derive and compute PCRLB with clutter and missed detections. As already derived in Chapter 4, under the linear system model (recalled that the nearly constant velocity (CV) system model is adopted throughout this thesis), the recursive form of the Fisher information matrix (FIM), $\mathbf{J}_k$ is given by[5]:

$$\mathbf{J}_k = \mathbf{D}_{k-1}^{22} - \mathbf{D}_{k-1}^{21}\left(\mathbf{J}_{k-1} + \mathbf{D}_{k-1}^{11}\right)^{-1}\mathbf{D}_{k-1}^{12} \tag{5.15}$$

where

$$\mathbf{D}_{k-1}^{11} = \mathbf{A}_{k-1}^{T}\mathbf{Q}_{k-1}^{-1}\mathbf{A}_{k-1} \tag{5.16}$$

[5] To keep the notational clarity in the derivation, here we assume that FIM $\mathbf{J}_{k-1}$ at the $(k-1)$-th time step is already known and derive the FIM $\mathbf{J}_k$ for the k-th time step.

$$\mathbf{D}_{k-1}^{12} = -\mathbf{A}_{k-1}^{T}\mathbf{Q}_{k-1}^{-1} \tag{5.17}$$

$$\mathbf{D}_{k-1}^{21} = -\mathbf{Q}_{k-1}^{-1}\mathbf{A}_{k-1}^{T} \tag{5.18}$$

$$\mathbf{D}_{k-1}^{22} = \mathbf{Q}_{k-1}^{-1} + E\left\{-\nabla_{\mathbf{x}_k}\nabla_{\mathbf{x}_k}^{T}\ln p\left(\mathbf{z}_k \mid \mathbf{x}_k\right)\right\} \tag{5.19}$$

In the above equations, only the second part of Equation 5.19 shows the dependency of the PCRLB on the measurement at the k-th time step, and only this part is affected by the measurement origin uncertainty due to clutter and missed detections. Therefore, we will focus on this part in the following derivation of the measurement contribution to the PCRLB under measurement origin uncertainty.

5.4.1 Derivation of the Measurement Contribution to the PCRLB under Measurement Origin Uncertainty

Firstly, let's define the second part of Equation 5.19 at the k-th time step as $\mathbf{J}_{\mathbf{z}}(k)$:

$$\begin{aligned}\mathbf{J}_{\mathbf{z}}(k) &= E\left\{-\nabla_{\mathbf{x}_k}\nabla_{\mathbf{x}_k}^{T}\ln p\left(\mathbf{z}_k \mid \mathbf{x}_k\right)\right\} \\ &= E\left\{\left[\nabla_{\mathbf{x}_k}\ln p\left(\mathbf{z}_k \mid \mathbf{x}_k\right)\right]\left[\nabla_{\mathbf{x}_k}\ln p\left(\mathbf{z}_k \mid \mathbf{x}_k\right)\right]^{T}\right\}\end{aligned} \tag{5.20}$$

Now the task is to derive $\mathbf{J}_{\mathbf{z}}(k)$, the measurement contribution to PCRLB at the k-th time step. As in Chapter 4, we assume that there are total N_s sensing nodes are activated to participate in the tracking task at the k-th time step. Thus the PCRLB will be the reverse of a mixture FIM of which each component corresponds to one of the N_s sensing nodes (refer to Section 4.10 of Chapter 4). In the following derivation, firstly we will derive $\mathbf{J}_{z}^{n}(k)$, the measurement contribution to the PCRLB from the n-th sensing node at the k-th time step and then extend the results to the N_s sensing nodes. Using notations described earlier in this chapter, the measurements obtained at the n-th sensing node is denoted as $\mathbf{Z}_k^n = \left(\mathbf{z}_{1,k}^n,...,\mathbf{z}_{j,k}^n,...,\mathbf{z}_{l_k^n,k}^n\right), \quad j = 1,...,l_k^n$, where l_k^n is the total number of measurements acquired by the n-th sensing node.

From the Equation 5.20, we can further write $\mathbf{J}_{z}^{n}(k)$ as follows:

$$
\begin{aligned}
\mathbf{J}_z^n(k) &= E\left\{\left[\nabla_{\mathbf{x}_k} \ln p\left(\mathbf{Z}_k^n \middle| \mathbf{x}_k\right)\right]\left[\nabla_{\mathbf{x}_k} \ln p\left(\mathbf{Z}_k^n \middle| \mathbf{x}_k\right)\right]^T\right\} \\
&= \sum_{l_k^n=1}^{\infty} P\left(l_k^n\right) E\left\{\left[\nabla_{\mathbf{x}_k} \ln p\left(\mathbf{Z}_k^n \middle| \mathbf{x}_k, l_k^n\right)\right]\left[\nabla_{\mathbf{x}_k} \ln p\left(\mathbf{Z}_k^n \middle| \mathbf{x}_k, l_k^n\right)\right]^T\right\} \\
&= \sum_{l_k^n=1}^{\infty} P\left(l_k^n\right) E\left\{\left[\nabla_{\mathbf{x}_k} \ln p\left(\left\{\mathbf{z}_{j,k}^n\right\}_{j=1}^{l_k^n} \middle| \mathbf{x}_k\right)\right]\left[\nabla_{\mathbf{x}_k} \ln p\left(\left\{\mathbf{z}_{j,k}^n\right\}_{j=1}^{l_k^n} \middle| \mathbf{x}_k\right)\right]^T\right\} \\
&= \sum_{l_k^n=1}^{\infty} P\left(l_k^n\right) \mathbf{J}_z^n\left(l_k^n\right)
\end{aligned}
\tag{5.21}
$$

where $P\left(l_k^n\right)$ is the prior probability that there are l_k^n measurements at the k-th time step and has been derived in Equation 5.6. $\mathbf{J}_z^n\left(l_k^n\right)$ is defined as

$$
\mathbf{J}_z^n\left(l_k^n\right) = E\left\{\left[\nabla_{\mathbf{x}_k} \ln p\left(\left\{\mathbf{z}_{j,k}^n\right\}_{j=1}^{l_k^n} \middle| \mathbf{x}_k\right)\right]\left[\nabla_{\mathbf{x}_k} \ln p\left(\left\{\mathbf{z}_{j,k}^n\right\}_{j=1}^{l_k^n} \middle| \mathbf{x}_k\right)\right]^T\right\} \tag{5.22}
$$

Recalled from Equations 5.8 and 5.9, $p\left(\left\{\mathbf{z}_{j,k}^n\right\}_{j=1}^{l_k^n} \middle| \mathbf{x}_k\right)$ in the above Equations is actually

$$
\begin{aligned}
p\left(\mathbf{Z}_k^n \middle| \mathbf{x}_k, l_k^n\right) &= p\left(\left\{\mathbf{z}_{j,k}^n\right\}_{j=1}^{l_k^n} \middle| \mathbf{x}_k\right) \\
&= \frac{\left[1-\varepsilon\left(l_k^n\right)\right]}{V^{l_k^n}} + \frac{\varepsilon\left(l_k^n\right)}{V^{l_k^n-1} l_k^n} \times \sum_{j=1}^{l_k^n} p\left(\mathbf{z}_{j,k}^n \middle| \mathbf{x}_k\right)
\end{aligned}
\tag{5.23}
$$

IN Equation 5.23, $\varepsilon\left(l_k^n\right)$ is the probability that a measurement is target generated and is given by Equation 5.7. $p\left(\mathbf{z}_{j,k}^n \middle| \mathbf{x}_k\right)$ is the probability density function of the measurement likelihood of the j-th measurement as defined in Equation 5.10. Substituting Equations 5.10 and 5.23 into Equation 5.22 and taking the gradient with respect to $\mathbf{x}_k$, we can get

$$
\begin{aligned}
\mathbf{J}_z^n\left(l_k^n\right) &= E\left\{\left[\nabla_{\mathbf{x}_k} \ln p\left(\left\{\mathbf{z}_{j,k}^n\right\}_{j=1}^{l_k^n} \middle| \mathbf{x}_k\right)\right]\left[\nabla_{\mathbf{x}_k} \ln p\left(\left\{\mathbf{z}_{j,k}^n\right\}_{j=1}^{l_k^n} \middle| \mathbf{x}_k\right)\right]^T\right\} \\
&= \left(\hat{\mathbf{H}}_k^n\right)^T \Psi_k^n\left(l_k^n\right) \hat{\mathbf{H}}_k^n
\end{aligned}
\tag{5.24}
$$

where $\hat{\mathbf{H}}_k^n$ is the Jacobian of the measurement function as defined in Equation 5.11 and $\Psi_k^n\left(l_k^n\right)$ is defined as

$$\Psi_k^n\left(l_k^n\right)=E\left\{\left[\sum_{j=1}^{l_k^n} f\left(\mathbf{z}_{j,k}^n,\mathbf{x}_k\right)\left(\mathbf{R}_k^n\right)^{-1}\left(\mathbf{z}_{j,k}^n-\hat{\mathbf{H}}_k^n\,\mathbf{x}_k\right)\right]\times\left[\sum_{j=1}^{l_k^n} f\left(\mathbf{z}_{j,k}^n,\mathbf{x}_k\right)\left(\mathbf{R}_k^n\right)^{-1}\left(\mathbf{z}_{j,k}^n-\hat{\mathbf{H}}_k^n\,\mathbf{x}_k\right)\right]^T\right\} \tag{5.25}$$

where

$$f\left(\mathbf{z}_{j,k}^n,\mathbf{x}_k\right)$$

$$=\frac{V\dfrac{\varepsilon\left(l_k^n\right)}{l_k^n}\dfrac{1}{\sqrt{\left|2\pi\mathbf{R}_k^n\right|}}\exp\left[-\frac{1}{2}\left(\mathbf{z}_{j,k}^n-\hat{\mathbf{H}}_k^n\,\mathbf{x}_k\right)^T\left(\mathbf{R}_k^n\right)^{-1}\left(\mathbf{z}_{j,k}^n-\hat{\mathbf{H}}_k^n\,\mathbf{x}_k\right)\right]}{\left(1-\varepsilon\left(l_k^n\right)\right)+V\dfrac{\varepsilon\left(l_k^n\right)}{l_k}\dfrac{1}{\sqrt{\left|2\pi\mathbf{R}_k^n\right|}}\sum_{j=1}^{l_k}\exp\left[-\frac{1}{2}\left(\mathbf{z}_{j,k}^n-\hat{\mathbf{H}}_k^n\,\mathbf{x}_k\right)^T\left(\mathbf{R}_k^n\right)^{-1}\left(\mathbf{z}_{j,k}^n-\hat{\mathbf{H}}_k^n\,\mathbf{x}_k\right)\right]} \tag{5.26}$$

For most applications, analytically calculating the expectation in Equation 5.26 is almost impossible and we need to resort to numerical methods which require further complicated mathematical derivations. To simplify the derivation of $\Psi_k^n\left(l_k^n\right)$ in Equation 5.25, two assumptions are made here:

Assumption 1: The integration region of the measurements obtained at an individual sensing node $\left\{\mathbf{z}_{j,k}^n\right\}$, $j=1,...,l_k^n$ is symmetric;

Assumption 2: The measurement noise is zero mean and its covariance $\mathbf{R}_k^n$ is a multiple of the identity matrix and takes the following form:

$$\mathbf{R}_k^n=\left(\sigma_k^n\right)^2\mathbf{I}_{n_\mathbf{n}} \tag{5.27}$$

Where $\mathbf{I}_{n_\mathbf{n}}$ is a $n_\mathbf{n}$ dimension identity matrix ($n_\mathbf{n}$ is the dimension of measurement noise) and σ_k^n is the standard deviation of the measurement noise at the n-th sensing node during the k-th time step.

Define

$$\tilde{\mathbf{z}}_{j,k}^n=\mathbf{z}_{j,k}^n-\hat{\mathbf{H}}_k^n\,\mathbf{x}_k,\quad j=1,...,l_k^n \tag{5.28}$$

From Assumption 2, the elements of a particular $\tilde{\mathbf{z}}_{j,k}^{n}$ are independently and identically distributed (i.i.d) with zero mean.

Substituting Equations 5.27 and 5.28 into Equation 5.25, $\Psi_k^n\left(l_k^n\right)$ becomes

$$\begin{aligned}\Psi_k\left(l_k^n\right) &= E\left\{\left[\sum_{j=1}^{l_k^n} f\left(\mathbf{z}_{j,k}^n,\mathbf{x}_k\right)\left(\sigma_k^n\right)^{-2}\left(\mathbf{z}_{j,k}^n-\hat{\mathbf{H}}_k^n\mathbf{x}_k\right)\right]\times\left[\sum_{j=1}^{l_k^n} f\left(\mathbf{z}_{j,k}^n,\mathbf{x}_k\right)\left(\sigma_k^n\right)^{-2}\left(\mathbf{z}_{j,k}^n-\hat{\mathbf{H}}_k^n\mathbf{x}_k\right)\right]^T\right\} \\ &= E\left\{\left[\sum_{j=1}^{l_k^n} f\left(\mathbf{z}_{j,k}^n,\mathbf{x}_k\right)^2\left(\sigma_k^n\right)^{-2}\left(\mathbf{z}_{j,k}^n-\hat{\mathbf{H}}_k^n\mathbf{x}_k\right)\left(\mathbf{z}_{j,k}^n-\hat{\mathbf{H}}_k^n\mathbf{x}_k\right)^T\left(\sigma_k^n\right)^{-2}\right]\right\} \\ &= \sum_{j=1}^{l_k^n} E\left\{\left(\sigma_k^n\right)^{-2} f\left(\tilde{\mathbf{z}}_{j,k}^n\right)^2\tilde{\mathbf{z}}_{j,k}^n\left(\tilde{\mathbf{z}}_{j,k}^n\right)^T\left(\sigma_k^n\right)^{-2}\right\}\end{aligned} \tag{5.29}$$

where

$$f\left(\tilde{\mathbf{z}}_{j,k}^n\right)=\frac{V\dfrac{\varepsilon\left(l_k^n\right)}{l_k^n}\dfrac{1}{\sqrt{2\pi}\left|\sigma_k^n\right|}\exp\left[-\dfrac{1}{2}\left(\tilde{\mathbf{z}}_{j,k}^n\right)^T\left(\sigma_k^n\right)^{-2}\tilde{\mathbf{z}}_{j,k}^n\right]}{\left(1-\varepsilon\left(l_k^n\right)\right)+V\dfrac{\varepsilon\left(l_k^n\right)}{l_k^n}\dfrac{1}{\sqrt{2\pi}\left|\sigma_k^n\right|}\displaystyle\sum_{j=1}^{l_k^n}\exp\left[-\dfrac{1}{2}\left(\tilde{\mathbf{z}}_{j,k}^n\right)^T\left(\sigma_k^n\right)^{-2}\tilde{\mathbf{z}}_{j,k}^n\right]} \tag{5.30}$$

In the first step of Equation 5.29, the cross terms are odd-symmetric around $\hat{\mathbf{H}}_k^n\mathbf{x}_k$. Based on Assumption 1, they are equal to zero because of the symmetric integration region of measurements $\left\{\mathbf{z}_{j,k}^n\right\}$, $j=1,...,l_k^n$. Substituting Equations 5.24, 5.29 and 5.30 into Equation 5.21, we obtain the measurement contribution to PCRLB which takes account of all measurements obtained by the n-th sensing node at the k-th time step:

$$\begin{aligned}\mathbf{J}_z^n(k) &= \sum_{l_k^n=1}^{\infty} P\left(l_k^n\right)\mathbf{J}_z^n\left(l_k^n\right) \\ &= \sum_{l_k^n=1}^{\infty} P\left(l_k^n\right)\left(\hat{\mathbf{H}}_k^n\right)^T\Psi_k^n\left(l_k^n\right)\hat{\mathbf{H}}_k^n \\ &= \sum_{l_k^n=1}^{\infty} P\left(l_k^n\right)\left(\hat{\mathbf{H}}_k^n\right)^T E\left\{\left(\sigma_k^n\right)^{-2} f\left(\tilde{\mathbf{z}}_{j,k}^n\right)^2\tilde{\mathbf{z}}_{j,k}^n\left(\tilde{\mathbf{z}}_{j,k}^n\right)^T\left(\sigma_k^n\right)^{-2}\right\}\hat{\mathbf{H}}_k^n \\ &= \sum_{l_k^n=1}^{\infty} P\left(l_k^n\right)\left(\hat{\mathbf{H}}_k^n\right)^T\left[\sum_{j=1}^{l_k^n}\mathbf{\Phi}_{j,k}^n\right]\left(\sigma_k^n\right)^{-2}\hat{\mathbf{H}}_k^n\end{aligned} \tag{5.31}$$

where

$$\mathbf{\Phi}_{j,k}^{n} = \left(\sigma_k^n\right)^{-2} E\left\{ f\left(\tilde{\mathbf{z}}_{j,k}^{n}\right)^2 \tilde{\mathbf{z}}_{j,k}^{n} \left(\tilde{\mathbf{z}}_{j,k}^{n}\right)^T \right\} \tag{5.32}$$

Under Assumption 2, the elements of vector $\tilde{\mathbf{z}}_{j,k}^{n}$ are identically and independently (i.i.d) distributed with zero mean and the integration region of each element of $\tilde{\mathbf{z}}_{j,k}^{n}$ in the expectation in 5.32 is symmetric about zero. This leads to the off-diagonal elements of $\mathbf{\Phi}_{j,k}^{n}$ in Equation 5.32 being all zero. Hence, $\mathbf{\Phi}_{j,k}^{n}$ is then an identity matrix multiplied by a scalar:

$$\mathbf{\Phi}_{j,k}^{n} = \phi_{j,k}^{n} \mathbf{I}_{n_\mathbf{n}}, \quad j = 1,...,l_k^n \tag{5.33}$$

where $\mathbf{I}_{n_\mathbf{n}}$ is a $n_\mathbf{n}$ dimensional identity matrix ($n_\mathbf{n}$ is the dimension of measurement noise) and $\phi_{j,k}^{n}$ is as follows

$$\phi_{j,k}^{n} = \left(\sigma_k^n\right)^{-2} E\left\{ f\left(\tilde{\mathbf{z}}_{j,k}^{n}\right)^2 \tilde{\mathbf{z}}_{j,k}^{n} \left(\tilde{\mathbf{z}}_{j,k}^{n}\right)^T \right\}, \quad j = 1,...,l_k^n \tag{5.34}$$

Moreover, according to Assumptions 1 and 2 and Equation 5.28, $\left\{ \tilde{\mathbf{z}}_{j,k}^{n} \right\}$, $j = 1,...,l_k^n$ are identically distributed. Therefore, we have $\phi_{1,k}^{n} = ... = \phi_{j,k}^{n} = ... = \phi_{l_k^n,k}^{n}$ and Equation 5.33 becomes

$$\mathbf{\Phi}_{1,k}^{n} = ... = \mathbf{\Phi}_{j,k}^{n} = ... = \mathbf{\Phi}_{l_k^n,k}^{n} = \phi_{1,k}^{n} \mathbf{I}_{n_\mathbf{n}} \tag{5.35}$$

Substituting 5.35 into 5.31, $\mathbf{J}_{\mathrm{z}}^{n}(k)$, the measurement contribution to the PCRLB from the n-th sensing node at the k-th time step can now be expressed as

$$\mathbf{J}_{\mathrm{z}}^{n}(k) = \sum_{l_k^n=1}^{\infty} P\left(l_k^n\right)\left(\hat{\mathbf{H}}_k^n\right)^T \left[l_k^n \times \mathbf{\Phi}_{1,k}^{n} \right]\left(\sigma_k^n\right)^{-2} \hat{\mathbf{H}}_k^n \tag{5.36}$$

Now the remaining task is to calculate $\mathbf{\Phi}_{1,k}^{n}$. However, it is difficult to analytically calculate the expectation in Equation 5.34. Following subsection will develop the approximation method to calculate $\mathbf{\Phi}_{1,k}^{n}$, and in turn, finally compute the PCRLB.

5.4.2 Numerical Calculation of PCRLB

Explicitly writing out the expectation for Equation 5.34, we have

$$\begin{aligned}\phi_{1,k}^{n} &= \left(\sigma_k^n\right)^{-2} E\left\{ f\left(\tilde{\mathbf{z}}_{j,k}^{n}\right)^2 \tilde{\mathbf{z}}_{j,k}^{n} \left(\tilde{\mathbf{z}}_{j,k}^{n}\right)^T \right\} \\ &= \left(\sigma_k^n\right)^{-2} \int_{\mathbf{x}_k} \int_{\tilde{\mathbf{z}}_{l_k^n,k}^{n} \in V} \cdots \int_{\tilde{\mathbf{z}}_{1,k}^{n} \in V} f\left(\tilde{\mathbf{z}}_{1,k}^{n}\right)^2 \times \tilde{\mathbf{z}}_{1,k}^{n} \times \left(\tilde{\mathbf{z}}_{1,k}^{n}\right)^T \\ &\quad \times p\left(\left\{\tilde{\mathbf{z}}_{j,k}^{n}\right\}_{j=1}^{l_k^n} \middle| \mathbf{x}_k \right) p\left(\mathbf{x}_k\right) d\tilde{\mathbf{z}}_{l_k^n,k}^{n} \ldots d\tilde{\mathbf{z}}_{1,k}^{n}\, d\mathbf{x}_k \end{aligned} \tag{5.37}$$

Note that Equation 5.37 is a $\left(l_k^n+1\right)$-fold integral with respect to $\mathbf{x}_k$ and $\tilde{\mathbf{z}}_{j,k}^{n}$, $j=1,\ldots,l_k^n$. Here we assume that the observation volume of the sensing node is large enough, and consequently, the inner integrations with respect to $\left\{\tilde{\mathbf{z}}_{j,k}^{n}\right\}_{j=1}^{l_k^n}$ are independent of $\mathbf{x}_k$ [118]. Consequently, in Equation 5.37 the integration with respect to $\mathbf{x}_k$ can be omitted. By substituting Equations 5.23 and 5.30 into 5.37, we have

$$\begin{aligned}\phi_{1,k}^{n} = \left(\sigma_k^n\right)^{-2} \int_{\tilde{\mathbf{z}}_{l_k^n,k}^{n} \in V} \cdots \int_{\tilde{\mathbf{z}}_{1,k}^{n} \in V} & \frac{\frac{1}{V^{l_k}} \left\{ V \frac{\varepsilon\left(l_k^n\right)}{l_k^n} \frac{1}{\sqrt{2\pi}\left|\sigma_k^n\right|} \exp\left[-\frac{1}{2} \left(\tilde{\mathbf{z}}_{1,k}^{n}\right)^T \left(\sigma_k^n\right)^{-2} \tilde{\mathbf{z}}_{1,k}^{n} \right] \right\}^2}{\left[1-\varepsilon\left(l_k^n\right)\right] + V \frac{\varepsilon\left(l_k^n\right)}{l_k^n} \frac{1}{\sqrt{2\pi}\left|\sigma_k^n\right|} \sum_{j=1}^{l_k^n} \exp\left[-\frac{1}{2} \left(\tilde{\mathbf{z}}_{j,k}^{n}\right)^T \left(\sigma_k^n\right)^{-2} \tilde{\mathbf{z}}_{j,k}^{n} \right]} \\ & \times \left(\tilde{\mathbf{z}}_{1,k}^{n}\right)^T \tilde{\mathbf{z}}_{1,k}^{n}\, d\tilde{\mathbf{z}}_{l_k^n,k}^{n} \ldots d\tilde{\mathbf{z}}_{1,k}^{n} \end{aligned} \tag{5.38}$$

To facility the integration in Equation 5.38, we assume that the measurements are restricted to a validation gate [118], [119]:

$$\left| \left(\tilde{\mathbf{z}}_{j,k}^{n} \right) \right| < g\,\sigma_k^n, \quad j=1,\ldots,l_k^n \tag{5.39}$$

where g is a constant controlling the gate volume. Now the observation volume V is replaced by the volume of the validation gate $V_g = \left(2g\sigma_k^n\right)^{\mathbf{n_z}}$, here $\mathbf{n_z}$ is the dimension of the measurement vector $\tilde{\mathbf{z}}_{j,k}^n$. Substituting Equation 5.34 into Equation 5.38, now we have

$$\begin{aligned}\phi_{1,k}^n = &\left(\sigma_k^n\right)^{-2}\int_{-g\sigma_1^n(1)}^{g\sigma_1^n(1)}\cdots\int_{-g\sigma_1^n(\mathbf{n_z})}^{g\sigma_1^n(\mathbf{n_z})}\cdots\int_{-g\sigma_k^n(1)}^{g\sigma_k^n(1)}\cdots\int_{-g\sigma_k^n(\mathbf{n_z})}^{g\sigma_k^n(\mathbf{n_z})}\frac{1}{V_g^{\,l_k^n}}\\
&\times\frac{\left\{V_g\dfrac{\varepsilon_g\left(l_k^n\right)}{l_k^n}\dfrac{1}{\sqrt{2\pi}\left|\sigma_k^n\right|}\exp\left[-\dfrac{1}{2}\left(\tilde{\mathbf{z}}_{1,k}^{\,n}\right)^T\left(\sigma_k^n\right)^{-2}\tilde{\mathbf{z}}_{1,k}^{\,n}\right]\right\}^2\left(\tilde{\mathbf{z}}_{1,k}^{\,n}\right)^T\tilde{\mathbf{z}}_{1,k}^{\,n}}{\left(1-\varepsilon_g\left(l_k^n\right)\right)+V_g\dfrac{\varepsilon_g\left(l_k^n\right)}{l_k^n}\dfrac{1}{\sqrt{2\pi}\left|\sigma_k^n\right|}\displaystyle\sum_{j=1}^{l_k^n}\exp\left[-\frac{1}{2}\left(\tilde{\mathbf{z}}_{j,k}^n\right)^T\left(\sigma_k^n\right)^{-2}\tilde{\mathbf{z}}_{j,k}^n\right]}d\tilde{\mathbf{z}}_{l_k^n,k}^{\,n}\ldots d\tilde{\mathbf{z}}_{1,k}^{\,n}\\
=&\frac{\left(\sigma_k^n\right)^{-2}\varepsilon_g\left(l_k^n\right)^2}{\left(l_k^n\right)^2\left(V_g\right)^{2l_k^n-2}\sqrt{2\pi}\left|\sigma_k^n\right|}\int_{-g\sigma_k^n}^{g\sigma_k^n}\cdots\int_{-g\sigma_k^n}^{g\sigma_k^n}\left(\tilde{\mathbf{z}}_{1,k}^{\,n}\right)^T\tilde{\mathbf{z}}_{1,k}^{\,n}\\
&\times\frac{\exp\left[-\dfrac{1}{2}\left(\tilde{\mathbf{z}}_{1,k}^{\,n}\right)^T\left(\sigma_k^n\right)^{-2}\tilde{\mathbf{z}}_{1,k}^{\,n}\right]}{\dfrac{1-\varepsilon_g\left(l_k^n\right)}{\left(V_g\right)^{l_k^n}}+\dfrac{\varepsilon_g\left(l_k^n\right)}{l_k^n\left(V_g\right)^{l_k^n-1}\sqrt{2\pi}\left|\sigma_k^n\right|}\displaystyle\sum_{j=1}^{l_k^n}\exp\left[-\frac{1}{2}\left(\tilde{\mathbf{z}}_{j,k}^n\right)^T\left(\sigma_k^n\right)^{-2}\tilde{\mathbf{z}}_{j,k}^n\right]}d\tilde{\mathbf{z}}_{l_k^n,k}^{\,n}\ldots d\tilde{\mathbf{z}}_{1,k}^{\,n}\end{aligned}\tag{5.40}$$

where

$$\varepsilon_g\left(l_k^n\right)=\frac{P_d}{P_g\left(l_k^n\right)}\frac{\left(\lambda V_g\right)^{l_k^n-1}\exp\left(-\lambda V_g\right)}{\left(l_k^n-1\right)!}\tag{5.41}$$

$$P_g\left(l_k^n\right)=\left(1-P_d\right)\frac{\left(\lambda V_g\right)^{l_k^n}\exp\left(-\lambda V_g\right)}{l_k^n!}+P_d\frac{\left(\lambda V_g\right)^{l_k^n-1}\exp\left(-\lambda V_g\right)}{\left(l_k^n-1\right)!}\tag{5.42}$$

In Equation 5.40, the $\int_{-g\sigma_1^n(1)}^{g\sigma_1^n(1)} \ldots \int_{-g\sigma_1^n(\mathbf{n_z})}^{g\sigma_1^n(\mathbf{n_z})}$ integral is taken over all components of $\mathbf{n_z}$ dimensional measurement vector $\tilde{\mathbf{z}}_{j,k}^n$ and this integral occurs l_k^n times (once for each measurement). If we let

$$\hat{\mathbf{z}}_{j,k}^n = \frac{\tilde{\mathbf{z}}_{j,k}^n}{\sigma_k^n}, \tag{5.43}$$

then Equation 5.40 can be simplified as

$$\phi_{1,k}^n = \frac{\left|\sigma_k^n\right|^{l_k^n-2} \varepsilon_g\left(l_k^n\right)^2}{\left(l_k^n\right)^2 \left(V_g\right)^{2l_k^n-2} 2\pi} \int_{-g}^{g}\ldots\int_{-g}^{g}\ldots\int_{-g}^{g}\ldots\int_{-g}^{g} \left(\hat{\mathbf{z}}_{1,k}^n\right)^T \hat{\mathbf{z}}_{1,k}^n \times \frac{\exp\left[-\frac{1}{2}\left(\hat{\mathbf{z}}_{1,k}^n\right)^T \left(\sigma_k^n\right)^{-2} \hat{\mathbf{z}}_{1,k}^n\right]}{\frac{1-\varepsilon_g\left(l_k^n\right)}{\left(V_g\right)^{l_k^n}} + \frac{\varepsilon_g\left(l_k^n\right)}{l_k^n \left(V_g\right)^{l_k^n-1}\sqrt{2\pi}\left|\sigma_k^n\right|} \sum_{j=1}^{l_k^n} \exp\left[-\frac{1}{2}\left(\hat{\mathbf{z}}_{j,k}^n\right)^T \left(\sigma_k^n\right)^{-2} \hat{\mathbf{z}}_{j,k}^n\right]} d\hat{\mathbf{z}}_{l_k^n,k}^n \ldots d\hat{\mathbf{z}}_{1,k}^n \tag{5.44}$$

The integration in Equation 5.44 can be solved by the Monte Carlo integration technique [131]. Finally, by substituting Equations 5.44, 5.35, 5.36 into 5.21, $\mathbf{J}_{\mathbf{z}}^n(k)$, the measurement contribution to the PCRLB from the n-th sensing node at the k-th time step can be obtained.

For N_s sensing nodes participating the tracking task, their measurements contribution to the PCRLB $\mathbf{J}_{\mathbf{z}}(k)$ cam then be written as follows

$$\begin{aligned}
\mathbf{J}_z(k) &= \sum_n^{N_s} \mathbf{J}_z^n(k) \\
&= \sum_n^{N_s} \sum_{l_k^n=1}^{\infty} P\left(l_k^n\right)\left(\hat{\mathbf{H}}_k^n\right)^T \left[l_k^n \times \phi_{1,k}^n\right]\left(\sigma_k^n\right)^{-2} \hat{\mathbf{H}}_k^n \\
&= \sum_n^{N_s} \left\{\sum_{l_k^n=1}^{\infty} P\left(l_k^n\right) \times l_k^n \times \phi_{1,k}^n\right\} \left(\hat{\mathbf{H}}_k^n\right)^T \left(\sigma_k^n\right)^{-2} \hat{\mathbf{H}}_k^n \\
&= \sum_n^{N_s} q_2^n \left(\hat{\mathbf{H}}_k^n\right)^T \left(\sigma_k^n\right)^{-2} \hat{\mathbf{H}}_k^n \\
&= \sum_n^{N_s} q_2^n \mathbf{J}_z^0(k)
\end{aligned} \tag{5.45}$$

where

$$q_2^n = \sum_{l_k^n=1}^{\infty} P_g\left(l_k^n\right) \times l_k^n \times \phi_{1,k}^n \tag{5.46}$$

$$\mathbf{J}_z^0(k) = \left(\hat{\mathbf{H}}_k^n\right)^T \left(\sigma_k^n\right)^{-2} \hat{\mathbf{H}}_k^n \tag{5.47}$$

In the literature, q_2^n is named as the *information reduction factor (IRF)*. $\mathbf{J}_z^0(k)$ is the counterpart of $\mathbf{J}_z(k)$ when there are no clutter and missed detections. Therefore, the measurement contribution to the PCRLB, $\mathbf{J}_z(k)$, can be regarded as the $\mathbf{J}_z^0(k)$ with no measurement origin uncertainty multiplied by a scalar IRF.

In Equations 5.45~5.47, $\mathbf{J}_z^0(k)$ can be readily obtained through the calculation of the Jacobian $\hat{\mathbf{H}}_k^n$ (refer to Section 4.10 in Chapter 4). The IRF q_2^n can be obtained through the computing of $\phi_{1,k}^n$ in Equation 5.44 by Monte Carlo approximation method as follows [131]:

$$\phi_{1,k}^n = \frac{(2g)^{l_k^n} \left|\sigma_k^n\right|^{l_k^n-2} \varepsilon_g\left(l_k^n\right)^2}{\left(l_k^n\right)^2 \left(V_g\right)^{2l_k^n-2} (2\pi)} \times \frac{1}{N_m} \sum_{l_k^n=1}^{N_m} \frac{\left[U_{1,1}(l)\right]^2 \exp\left\{-\sum_{i=1}^{n_{\mathbf{z}}} \left[U_{1,i}(l)\right]^2\right\}}{\frac{1-\varepsilon_g\left(l_k^n\right)}{\left(V_g\right)^{l_k^n}} + \frac{\varepsilon_g\left(l_k^n\right)}{l_k^n \left(V_g\right)^{l_k^n-1} \sqrt{2\pi}\left|\sigma_k^n\right|} \sum_{j=1}^{l_k^n} \exp\left\{-\frac{1}{2}\sum_{r=1}^{n_{\mathbf{z}}} \left[U_{j,r}(l)\right]^2\right\}} \tag{5.48}$$

where $U_{j,r}(l)$, $j=1,...,l_k^n$; $r=1,...,n_{\mathbf{z}}$; $l=1,...,N_m$ are independent and identically distributed random variables drawn from a uniform distribution on $[-g,g]$. From Equations 5.42, 5.46 and 5.48, it can been seen that IRF q_2^n will be time invariant if the measurement noise, the clutter rate, and the detection rate are remain unchanged over time steps throughout the tracking task. This implies that we only need to calculate q_2 once.

As in Chapter 4, the target state estimate at the previous time step is needed for computing the FIM $\mathbf{J}_k$ at the current time step. We still adopt particles' representation of the target state to compute the Jacobian $\hat{\mathbf{H}}_k$ as follows:

$$\hat{\mathbf{H}}_k^n = \begin{pmatrix} \dfrac{-2S\left(x_k^i - x_k^n\right)}{\left(x_k^i - x_k^n\right)^2 + \left(y_k^i - y_k^n\right)^2} \\ 0 \\ \dfrac{-2S\left(y_k^i - y_k^n\right)}{\left(x_k^i - x_k^n\right)^2 + \left(y_k^i - y_k^n\right)^2} \\ 0 \end{pmatrix}^T \tag{5.49}$$

where S is the target energy and set to $S = 5000$ as in the simulations. $\left(x_k^n, y_k^n\right)$ and $\left(x_k^i, y_k^i\right)$ are the positions of the n-th sensing node's and the i-th particle's position at the k-th time step, respectively.

Taking into account that total N_s sensing nodes participating the tracking task, we need to substitute Equation 5.49 into Equation 5.45 to compute the measurement contribution $\mathbf{J}_z(k)$ to the PCRLB as follows:

$$\mathbf{J}_z(k) = \begin{pmatrix} \tau_k^{11} & 0 & \tau_k^{13} & 0 \\ 0 & 0 & 0 & 0 \\ \tau_k^{31} & 0 & \tau_k^{33} & 0 \\ 0 & 0 & 0 & 0 \end{pmatrix} \tag{5.50}$$

where τ_k^{11}, $\tau_k^{13} = \tau_k^{31}$, τ_k^{33} are given as below

$$\tau_k^{11} = \frac{1}{N\,\mathbf{R}_k} \left\{ \sum_{i=1}^{N} \sum_{n=1}^{N_s} q_2 \times \frac{4S^2\left(x_k^i - x_k^n\right)^2}{\left[\left(x_k^i - x_k^n\right)^2 + \left(y_k^i - y_k^n\right)^2\right]^2} \right\} \tag{5.51}$$

$$\tau_k^{13} = \frac{1}{N\,\mathbf{R}_k} \left\{ \sum_{i=1}^{N} \sum_{n=1}^{N_s} q_2 \times \frac{4S^2\left(x_k^i - x_k^n\right)\left(y_k^i - y_k^n\right)}{\left[\left(x_k^i - x_k^n\right)^2 + \left(y_k^i - y_k^n\right)^2\right]^2} \right\} \tag{5.52}$$

$$\tau_k^{33} = \frac{1}{N\,\mathbf{R}_k} \left\{ \sum_{i=1}^{N} \sum_{n=1}^{N_s} q_2 \times \frac{4S^2\left(y_k^i - y_k^n\right)^2}{\left[\left(x_k^i - x_k^n\right)^2 + \left(y_k^i - y_k^n\right)^2\right]^2} \right\} \tag{5.53}$$

In Equations 5.51~5.53, we make use of the relationship of $\mathbf{R}_k^n = \left(\sigma_k^n\right)^2$. The superscript n is removed for both measurement noise covariance $\mathbf{R}_k^n$ and IRF q_2^n since we

adopt the homogeneous sensing nodes with identical properties. It is needed to emphasize that IRF q_2 is a scalar and only needs to be computed once if the measurement noise, the clutter rate and the detection rate of the sensing nodes are time invariant.

Combining Equations 5.50~5.53 with Equations 5.15 ~ 5.20, we can finally obtain the PCRLB under measurement origin uncertainty due to clutter and missed detections for tracking a single target in the wireless sensor networks.

5.5 Simulations

This section evaluates the performance of PF-PDAF algorithm for single target tracking under measurement origin uncertainty in a wireless sensor network. The simulations are conducted under different tracking conditions including the clutter rate, the detection rate, the signal to noise ratio (SNR), the prior estimate of the target state and the number of particles used in the algorithm. The numeric results of root square PCRLB are also presented and compared with the RMSE of PF-PDAF algorithm under the same tracking conditions.

5.5.1 Simulation Setup

The simulation setup is chosen to the same as Chapter 4 as much as possible. The ground vehicle traverses through a two-dimensional (2D) sensor field and four different tracking scenarios are used in the simulation (Figure 5.1, a repeat of four tracking scenarios of Figure 4.3 in Chapter 4). These tracking scenarios are synthesized with different target trajectories, target dynamics, clutter rates, detection rates and sensing nodes. The target trajectories are digested from a real on-site experiment (details can be found in [23]).

In the simulation presented following, it is assumed that the tracking task is performed within one sensor cluster which consists of one cluster leader (not drawn in Figure 5.1) and a fixed set of 20 sensing nodes (active sensing nodes) selected from 200 randomly deployed sensing nodes. In the simulations conducted in Chapter 4, these 20 active sensing nodes are all activated to sense and transmit their measurements to the cluster leader for the target state estimate throughout the tracking task. However, in the simulations conducted in this chapter the cluster leader further selects first three sensing nodes that closest to the predicted target position from the 20 active sensing nodes, and only these three sensing nodes are activated to sense and transmit their measurements to the cluster leader. Upon

receiving the measurements from these three sensing nodes, the cluster leader then executes the PF-PDAF algorithm to update the target state estimate.

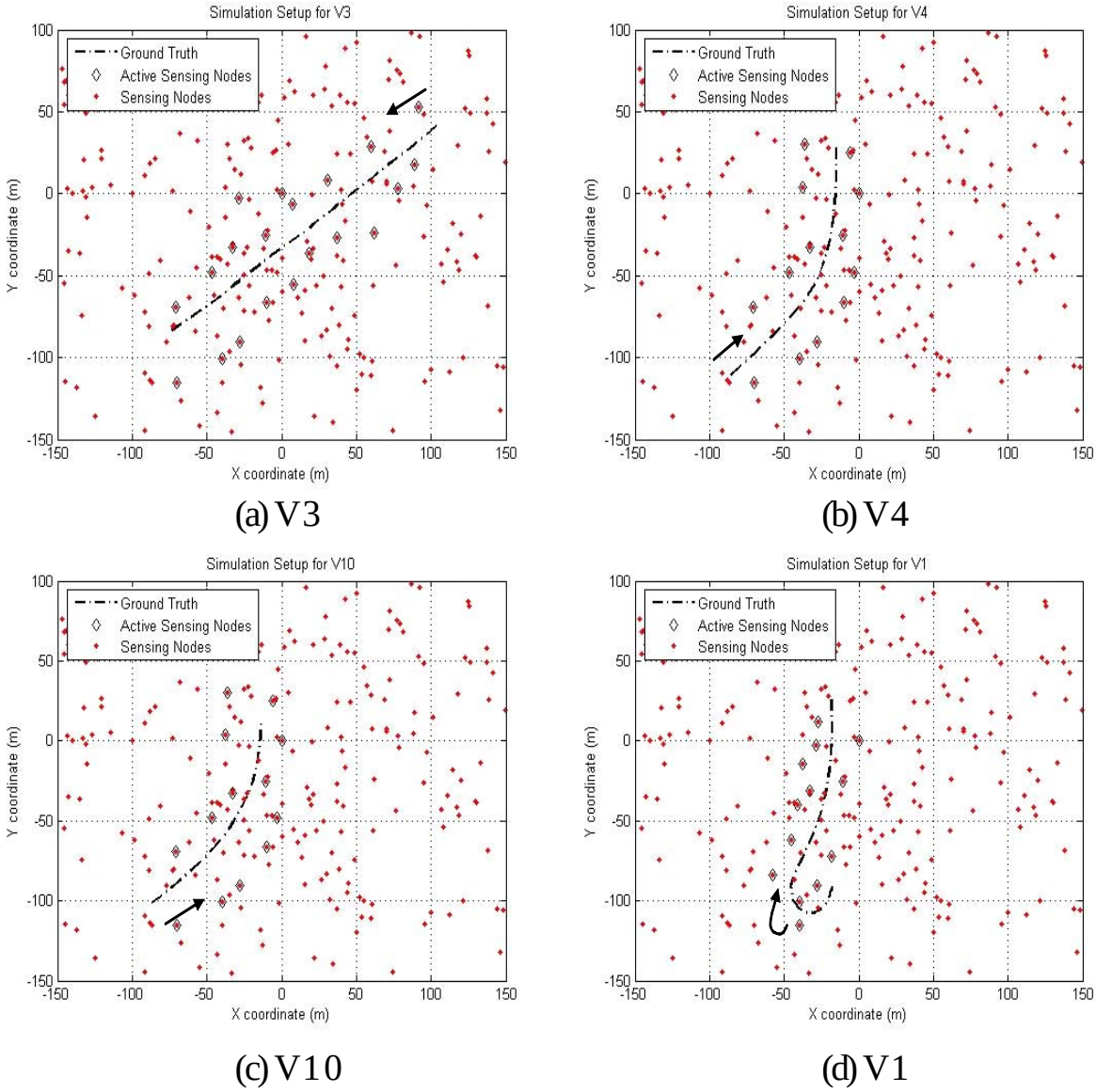

Figure 5.1 Four tracking scenarios with different target trajectories, target dynamics and active sensing nodes (V3, V4, V10 and V1 denote the four tracking scenarios)

The target originated measurement at each active sensing node is synthesized according to the measurement model defined in Equation 5.3. At the k-th time step, the target originated measurement at the n-th sensing node is as follows

$$\xi_{t,k}^{n} = \frac{S}{\left(x_k - x_n\right)^2 + \left(y_k - y_n\right)^2} + \varepsilon_k^n \tag{5.54}$$

where (x_k, y_k) and (x_n, y_n) are positions of the target and the n-th sensing node in x- and y-coordinate, respectively. S is the source energy and it is the acoustic intensity measured at 1 m away from the target. In the simulations, S is set to 5000 and the background noise is assumed to be Gaussian and set to $\varepsilon_k^n \sim N(0,1),\ n = 1, 2, ..., N_s$ for all active sensing nodes. The SNR is 37 dB at the target position, and actual SNR at a sensing node relies on the distance between this sensing node and the target. For example, for a sensing node that is 50 meters away from the target, the SNR is 10 dB.

Throughout this chapter, the assumption has been made that the measurement range of the sensing node is 100 meters. In the simulations, the clutter originated measurements obtained at a sensing node are synthesised independently and uniformly and are distributed in a square with the size of 200 m × 200 m, centered at the location of this sensing node. The number of clutter originated measurements follows the Poisson distribution as defined in Equation 5.5. The magnitude of the clutter originated measurements is set as the same as that of the target, i.e. 5000 and the noise level is also assumed to be Gaussian and set to $N(0,1)$. By assuming the same magnitude for the measurements originated from the target and from clutter, the difficulty of recognizing the origins of the measurements is greatly increased; hence we can assess the PF-PDAF algorithm's ability in effectively solving the data association problem.

The prior estimate of the target state is assumed to be Gaussian with mean $\mathbf{x}_{0|0}$ and covariance $\mathbf{P}_{0|0}$. To describe the different levels of the uncertainty in the prior knowledge regarding the target state, $\mathbf{x}_{0|0}$ and $\mathbf{P}_{0|0}$ are categorized into following three groups:

$$\mathbf{x}_{0|0}^1 = \mathbf{x}_{truth} + \begin{pmatrix} 15 \\ 0 \\ 15 \\ 0 \end{pmatrix}, \qquad \mathbf{P}_{0|0}^1 = \begin{pmatrix} 10 & 0 & 0 & 0 \\ 0 & 10 & 0 & 0 \\ 0 & 0 & 10 & 0 \\ 0 & 0 & 0 & 10 \end{pmatrix} \tag{5.55}$$

$$\mathbf{x}_{0|0}^2 = \mathbf{x}_{truth} + \begin{pmatrix} 5 \\ 0 \\ 5 \\ 0 \end{pmatrix}, \qquad \mathbf{P}_{0|0}^2 = \begin{pmatrix} 2 & 0 & 0 & 0 \\ 0 & 2 & 0 & 0 \\ 0 & 0 & 2 & 0 \\ 0 & 0 & 0 & 2 \end{pmatrix} \tag{5.56}$$

$$\mathbf{x}_{0|0}^3 = \mathbf{x}_{truth} + \begin{pmatrix} 1 \\ 0 \\ 1 \\ 0 \end{pmatrix}, \qquad \mathbf{P}_{0|0}^3 = \begin{pmatrix} 1 & 0 & 0 & 0 \\ 0 & 1 & 0 & 0 \\ 0 & 0 & 1 & 0 \\ 0 & 0 & 0 & 1 \end{pmatrix} \tag{5.57}$$

where $\mathbf{x}_{truth}$ is the ground truth at time step $k = 0$ (i.e. the initial position of the target).

In the simulations, 100 independent Monte Carlo runs have been conducted for the each setting of PF-PDAF algorithm and the RMSE is used to evaluate the performance of PF-PDAF algorithm. As in Chapter 4, two different types of RMSE are computed: one is averaged over all time steps for each individual Monte Carlo run, and another is averaged over all 100 Monte Carlo runs for each time step. These two types of RMSE are defined as below:

$$\text{RMSE}^{\,n} = \sqrt{\frac{1}{K}\sum_{k=1}^{K} \left\| \mathbf{r}_k^{\,n} - \hat{\mathbf{r}}_k^{\,n} \right\|^2} \tag{5.58}$$

$$\text{RMSE}_{\,k} = \sqrt{\frac{1}{\Phi}\sum_{n=1}^{\Phi} \left\| \mathbf{r}_k^{\,n} - \hat{\mathbf{r}}_k^{\,n} \right\|^2} \tag{5.59}$$

In Equation 5.58, $\text{RMSE}^{\,n}$ is referred to as the RMSE value of the n-th Monte Carlo run that is averaged over all time steps of the tracking task. K is the total number of time steps in the tracking task. $\mathbf{r}_k^n = \begin{bmatrix} x_k^n & y_k^n \end{bmatrix}^T$ and $\hat{\mathbf{r}}_k^n = \begin{bmatrix} \hat{x}_k^n & \hat{y}_k^n \end{bmatrix}^T$ correspond to the true target position and the estimated target position at the k-th time step during the n-th Monte Carlo run, respectively. In Equation 5.59, $\text{RMSE}_{\,k}$ is referred to as the RMSE value of the k-th time step that is averaged over 100 Monte Carlo runs. Φ is the total number of Monte Carlo runs (i.e. $\Phi = 100$). $\mathbf{r}_k^n = \begin{bmatrix} x_k^n & y_k^n \end{bmatrix}^T$ and $\hat{\mathbf{r}}_k^n = \begin{bmatrix} \hat{x}_k^n & \hat{y}_k^n \end{bmatrix}^T$ correspond to the true target position and the estimated target position in the n-th Monte Carlo run at the k-th time step, respectively.

5.5.2 PF-PDAF Results

The following graphs show the simulation results of PF-PDAF algorithm under various settings such as the clutter rate, the detection rate, the prior estimate of target state, the SNR and the particles number. In the simulations, the SNR is set to 37 dB at the target position. The prior estimate of the target state is Gaussian with the mean $\mathbf{x}_{0|0}^3$ and covariance $\mathbf{P}_{0|0}^3$ as defined in Equation 5.57. The number of particles adopted in the PF-PDAF algorithm is 1000.

Figure 5.2 depicts the RMSE values of tracking scenario V3 under the varying detection rates, i.e. $\mathrm{Pd} = 1, 0.9, 0.8, 0.7$ when the clutter rate λ is fixed such that $\mathrm{Cd} = \lambda V = 0.5$ ($\mathrm{Cd} = \lambda V$ is the averaged number of clutter originated measurements in the observation space V of a sensing node). Figure 5.2 (a) shows the RMSE_k value that averaged over all 100 independent Monte Carlo runs. Figure 5.2 (b) also shows the RMSE_k value; however, instead of being averaged over all 100 runs, the RMSE_k in Figure 5.2 (b) is computed by excluding the bottom 25 runs with the lowest RMSE^n and the top 25 runs with the largest RMSE^n (this is referred to as the processed data in the figure). The purpose of this data exclusion is to reduce the bias imposed by very large or very small RMSE values. Figures 5.2 (c) and 5.2 (d) are the RMSE^n values which are averaged over all time steps in the tracking task.

Figure 5.3 depicts the RMSE value of tracking scenario V3 under the varying clutter rates, i.e. $\mathrm{Cd} = 0.1, 0.5, 1.0, 1.5$ when the detection rate is fixed at $\mathrm{Pd} = 0.9$. Figure 5.3 (a) shows the RMSE_k value that averaged over all 100 independent runs, and Figure 5.3 (b) shows the RMSE_k value which is calculated by the data exclusion (e.g., similar to Figure 5.2 (b)). Figures 5.3 (c) and 5.3 (d) are the RMSE^n values which are averaged over all time steps in the tracking task.

From Figures 5.2 and 5.3, it can be seen that, as expected, increasing clutter rate or decreasing detection rate (i.e. the probability of missed detection increasing) leads to the deterioration in the tracking performance of PF-PDAF algorithm. For example, when the detection rate is decreased to $\mathrm{Pd} = 0.7$, 44 runs out of total 100 runs are divergent (the magnitude of RMSE^n is greater than 50 m in the particular run); and when the clutter rate is increased to $\mathrm{Cd} = 1.5$, 42 runs out of total 100 runs are divergent.

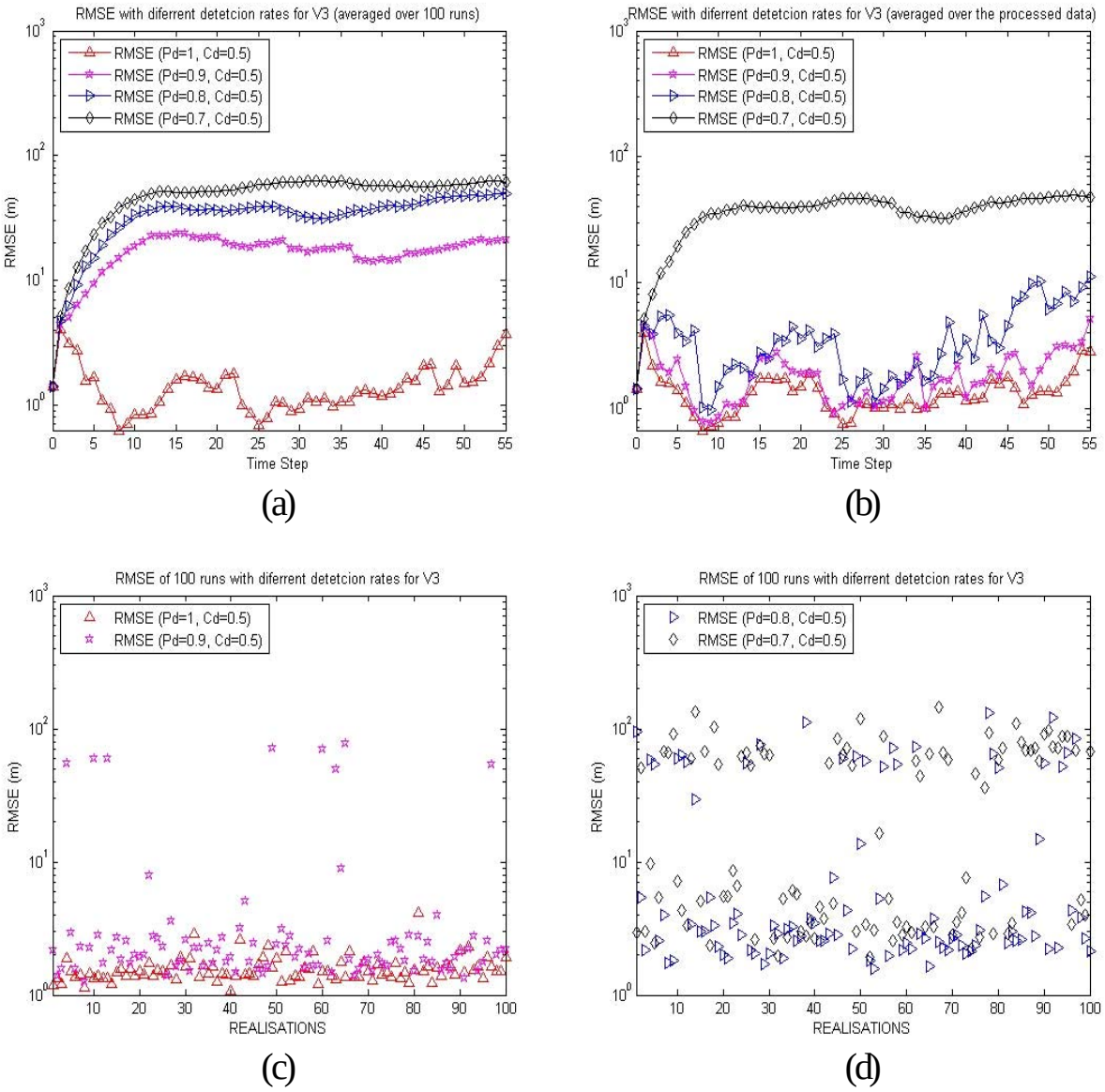

Figure 5.2 RMSE of PF-PDAF algorithm with varying detection rates for tracking scenario V3 (clutter rate fixed)

(a) RMSE_k value (averaged over all 100 runs)

(b) RMSE_k value (averaged over the processed data)

(c) RMSE^n value of 100 runs ($\text{Pd} = 1, \text{Cd} = 0.5$ and $\text{Pd} = 0.9, \text{Cd} = 0.5$)

(d) RMSE^n value of 100 runs ($\text{Pd} = 0.8, \text{Cd} = 0.5$ and $\text{Pd} = 0.7, \text{Cd} = 0.5$)

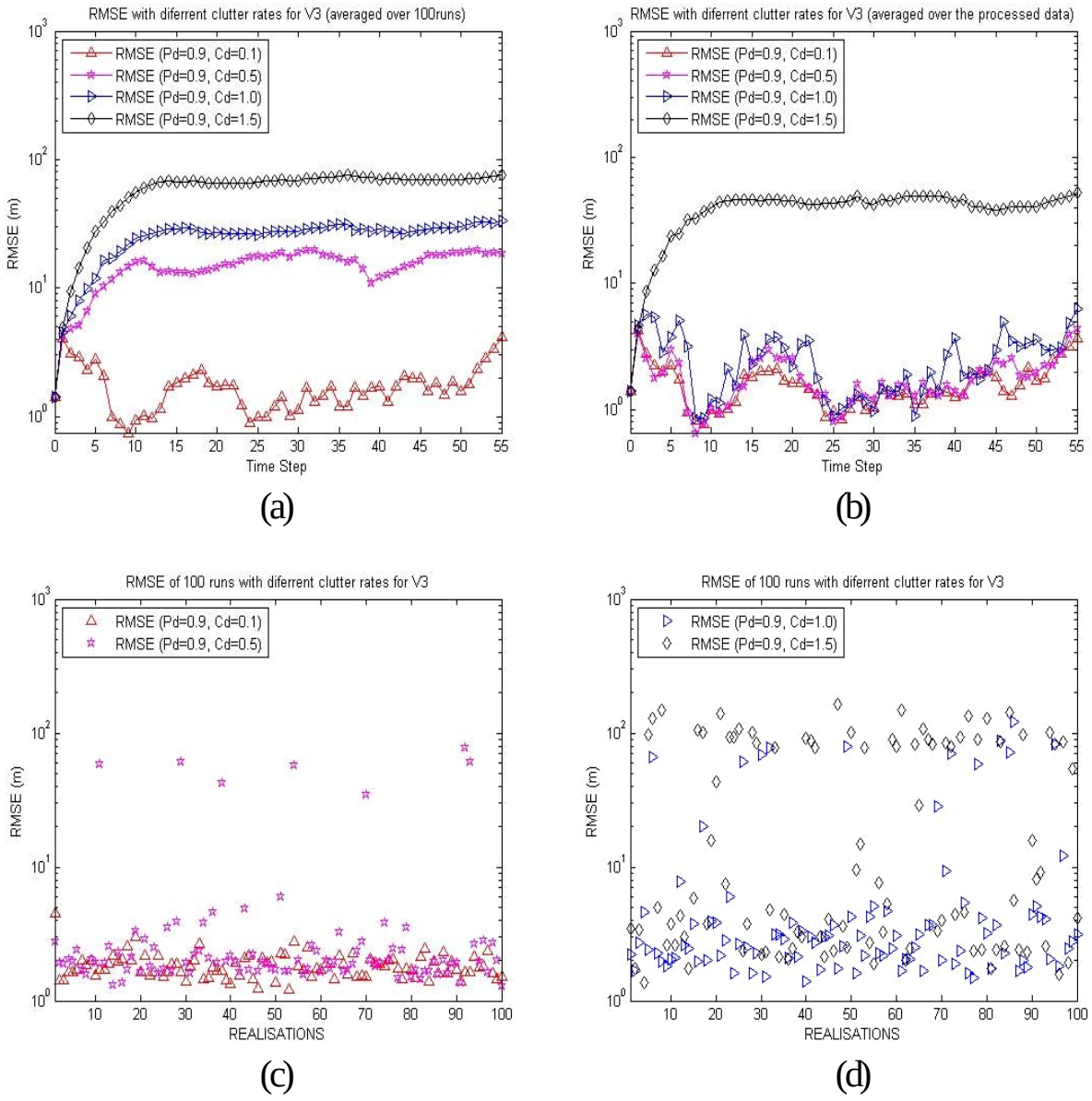

Figure 5.3 RMSE of PF-PDAF algorithm with varying clutter rates for tracking scenario V3 (detection rate fixed)

(a) RMSE_k value (averaged over all 100 runs)

(b) RMSE_k value (averaged over the processed data)

(c) RMSE^n value of 100 runs ($\text{Pd} = 0.9, \text{Cd} = 0.1$ and $\text{Pd} = 0.9, \text{Cd} = 0.5$)

(d) RMSE^n value of 100 runs ($\text{Pd} = 0.9, \text{Cd} = 1.0$ and $\text{Pd} = 0.9, \text{Cd} = 1.5$)

Figures 5.4 and 5.5 present the tracking performance of PF-PDAF algorithm under three different sets of clutter rates and detection rates, i.e. $\text{Pd} = 1, \text{Cd} = 0.01$, $\text{Pd} = 0.9, \text{Cd} = 0.5$, $\text{Pd} = 0.8, \text{Cd} = 1.0$ for each of the four tracking scenarios as depicted in Figure 5.1. Figure 5.4 shows the RMSE_k value which is computed under the above three sets of clutter rates

and detection rates. Figure 5.5 also shows the RMSE_k values, however, it is computed by the exclusion of bottom 25 runs with the lowest RMSE^n values and the top 25 runs with the largest RMSE^n values. In the above figures, the particles used in the simulations are 1000 except for tracking scenario V1 in which 2000 particles are used to cater for the extra tracking difficulty due to the "U" curve of the target trajectory (Figure 5.1(d)). The SNR and the prior estimate of target state remain the same as in Figures 5.2 and 5.3.

It is evidenced again from Figures 5.4 and 5.5 that the more measurement origin uncertainty imposed on the sensing nodes the more degradation on the tracking accuracy of the PF-PDAF algorithm occurs.

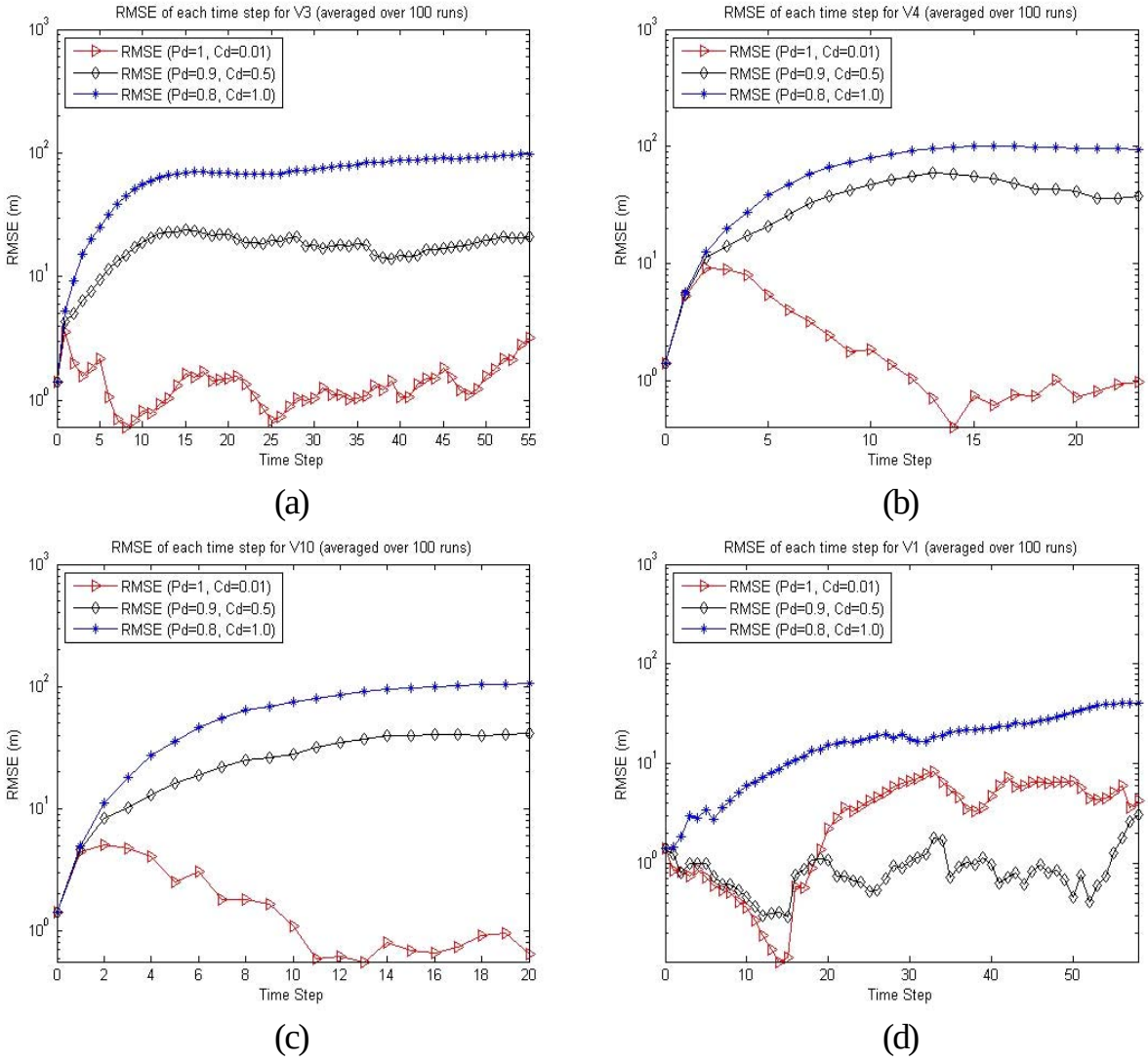

Figure 5.4 RMSE_k values of PF-PDAF algorithm for the four tracking scenarios (averaged over 100 runs)
(a) V3 (b) V4 (c) V10 (d) V1

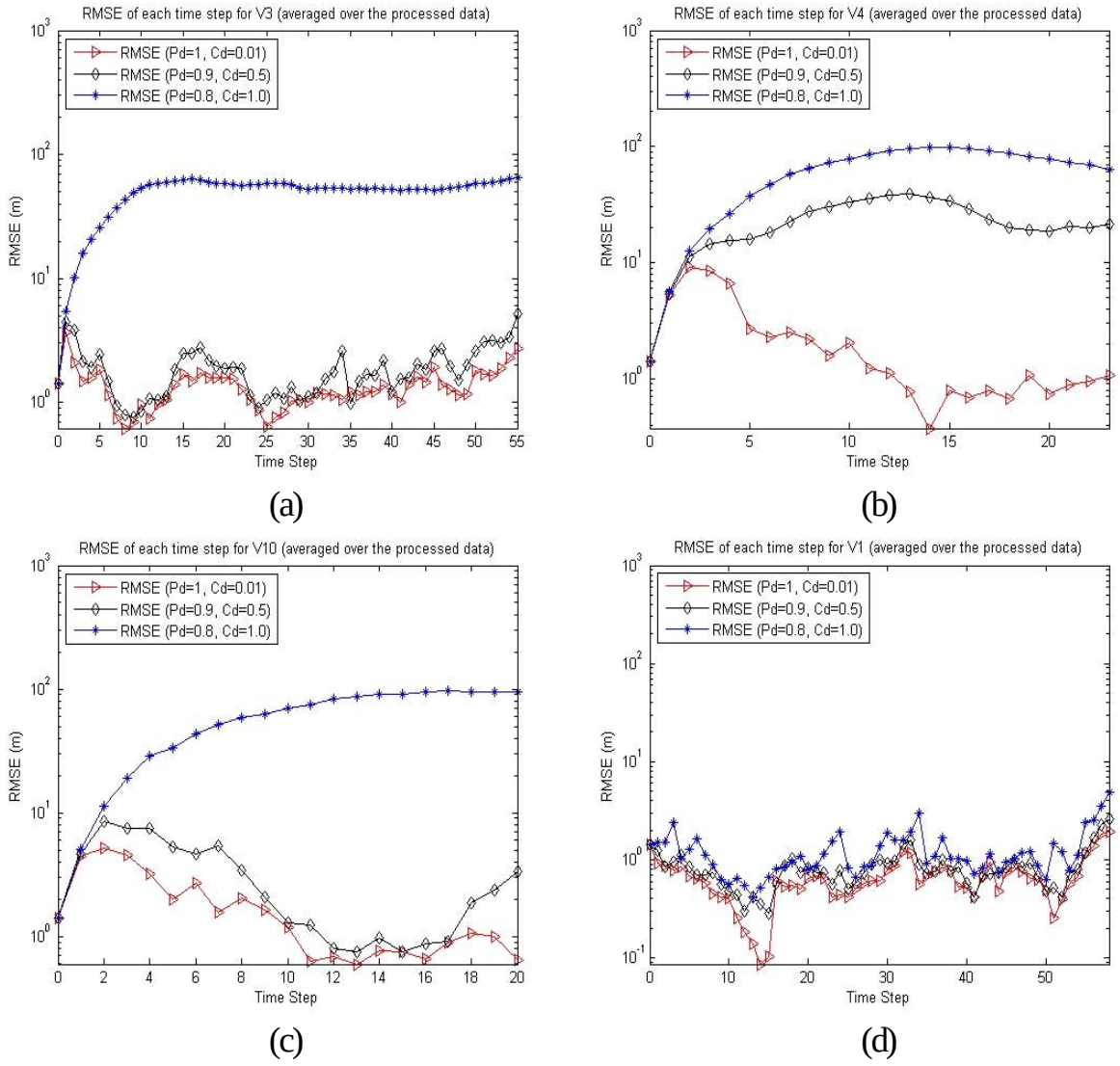

Figure 5.5 RMSE_k values of PF-PDAF algorithm for the four tracking scenarios (averaged over the processed data)
(a) V3 (b) V4 (c) V10 (d) V1

Figure 5.6 depicts the tracking performance of PF-PDAF algorithm under different SNR settings with the clutter and detection rates of $\mathrm{Pd} = 0.9,\ \mathrm{Cd} = 0.5$ for the tracking scenario V3. The prior estimate of the target state is Gaussian with the mean $\mathbf{x}_{0|0}^{3}$ and covariance $\mathbf{P}_{0|0}^{3}$ and the particle number is 1000. Figure 5.6 (a) shows the RMSE_k value which is averaged over all 100 runs while Figure 5.6 (b) shows the RMSE_k value that is computed by excluding the bottom 25 runs with the lowest RMSE^n values and top 25 runs with the largest RMSE^n values. Figures 5.6 (c) and 5.6 (d) are the RMSE^n value of all 100 independent runs. It can be observed that in general, higher SNRs lead to more accurate the

PF-PDAF algorithm. However, the magnitude of RMSE_k values under SNR 30 dB becomes close to that under SNR 27 dB. This is because many runs of PF-PDAF algorithm under SNR 30 dB have very high RMSE values (Figure 5.6 (d)). Such phenomena is caused by the adoption of transition prior as proposal distribution in the PF-PDAF algorithm, in which the particles are driven by the process noise in the system model to move from the $(k-1)$-th time step to the k-th time step in the state space; and very low noise levels (high SNRs) prevent particles from moving to the high measurement likelihood areas of the state space. In turn, the performance of the PF-PDAF algorithm is affected and its RMSE values are not well bounded. This implies that we need to design a better proposal distribution for PF-PDAF algorithm. However, as pointed out in Section 5.3, it is not a trivial task to design such a better proposal distribution under the measurement origin uncertainty.

Figure 5.7 shows the performance of PF-PDAF performance under three different sets of prior estimates of target state for tracking scenarios V3. These prior estimates are referred to as the uncertainty high (defined by Equations 5.55), the uncertainty medium (defined by Equations 5.56), the uncertainty low (defined by Equations 5.57). The SNR is set to 37 dB at the target position and the particle number is 1000. It can be seen that the increasing uncertainty in the prior estimate of target state will generally decrease the performance of PF-PDAF algorithm. However, the difference of the tracking accuracy under the medium uncertainty of prior target state estimate and the low uncertainty of prior target state estimate is not very dramatic. This is because now the dominate factor deciding the tracking accuracy of PF-PDAF LGORITHM is the level of measurement origin uncertainty, i.e., the clutter rates and the detection rates.

Figure 5.8 shows the RMSE value of PF-PDAF algorithm with different particles number for tracking scenario V3 under the setting of $\text{Pd} = 0.9, \text{Cd} = 0.5$, SNR 37 dB and the mean $\mathbf{x}_{0|0}^{3}$ and covariance matrix $\mathbf{P}_{0|0}^{3}$ of the prior estimate of target state. It can be seen that the increasing particles number lead to better tracking performance. However, the increase of the particles number comes with the higher cost in computation and may not be favored in the resources constrained wireless sensor networks.

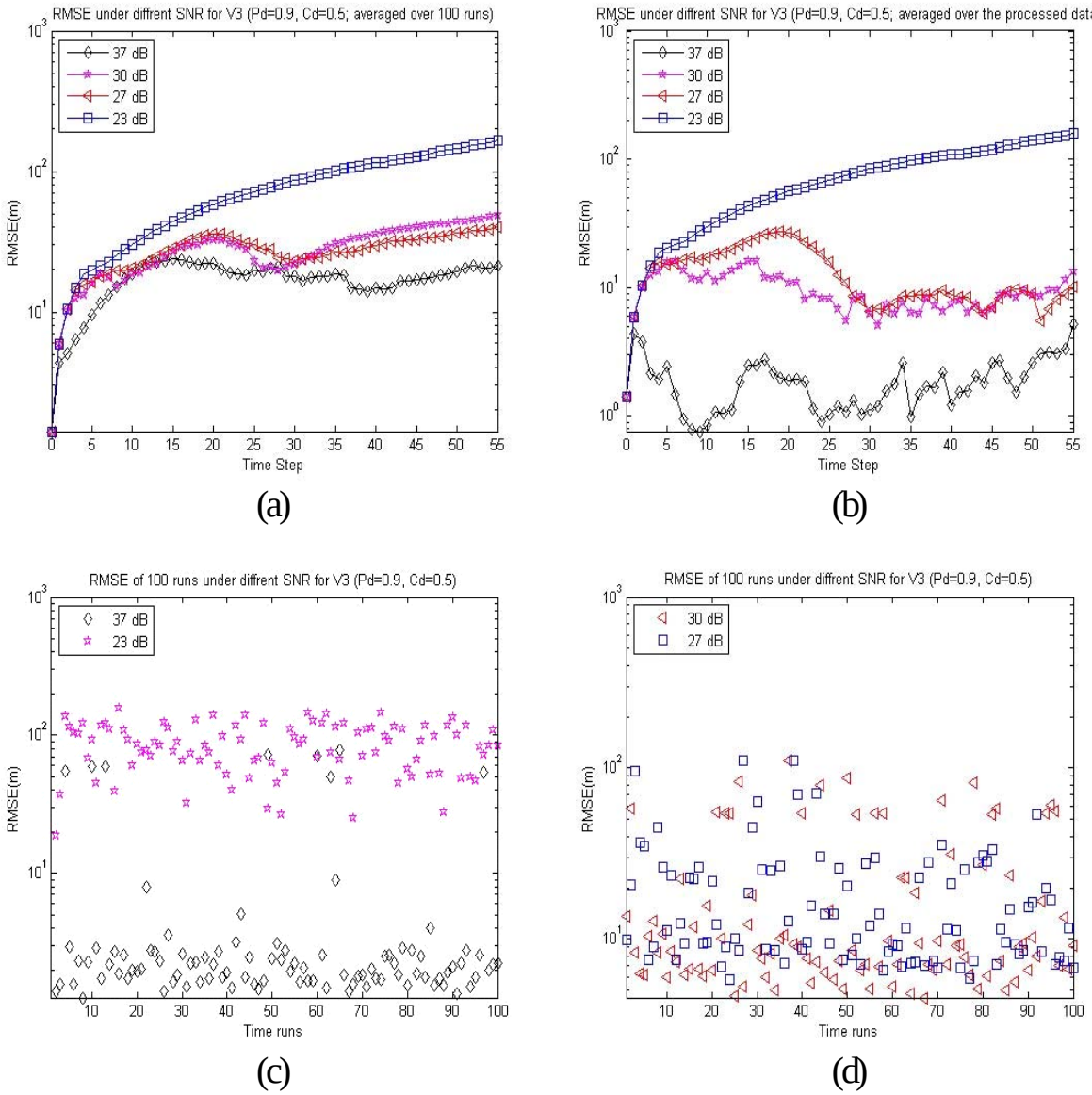

Figure 5.6 RMSE of PF-PDAF algorithm under different SNR for tracking scenario V3 ($Pd = 0.9, Cd = 0.5$, total 100 runs)

(a) $RMSE_k$ value (averaged over 100 runs)

(b) $RMSE_k$ value (averaged over the processed data)

(c) $RMSE^n$ value of 100 runs for SNR 37 dB and 23 dB

(d) $RMSE^n$ value of 100 runs for SNR 30 dB and 27 dB

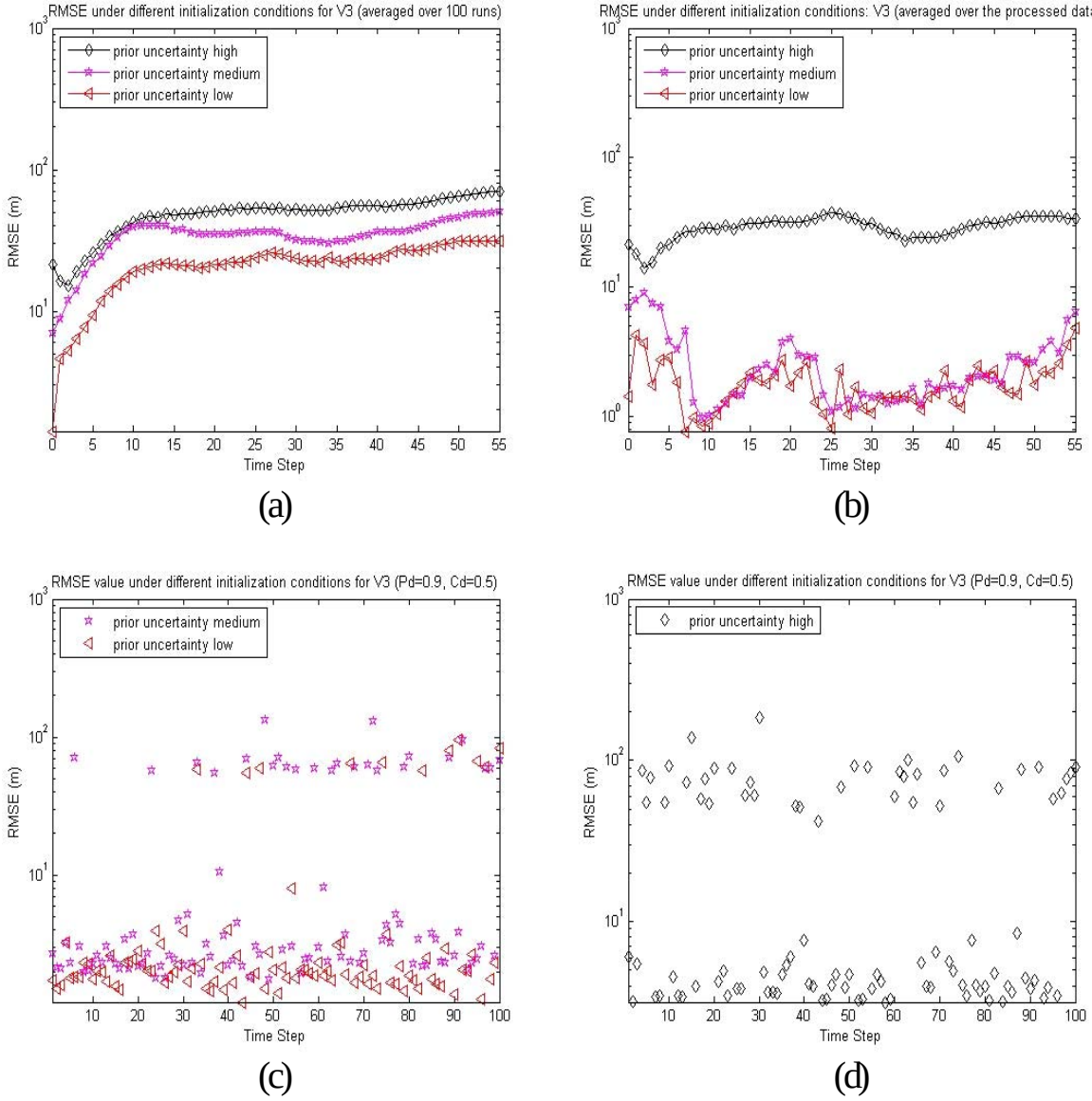

Figure 5.7 RMSE of PF-PDAF algorithm under different prior estimate of target state for tracking scenario V3 (Pd = 0.9, Cd = 0.5, total 100 runs)

(a) RMSE_k value (averaged over 100 runs)

(b) RMSE_k value (averaged over the processed data)

(c) RMSE^n of 100 runs with prior estimate uncertainties low and medium

(d) RMSE^n of 100 runs with prior estimate uncertainty high

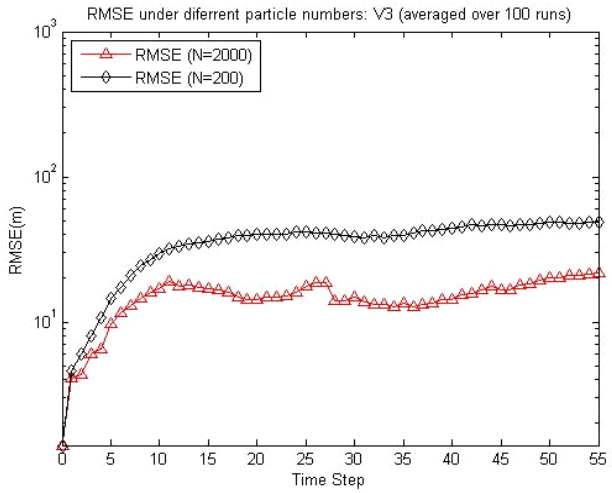

(a)

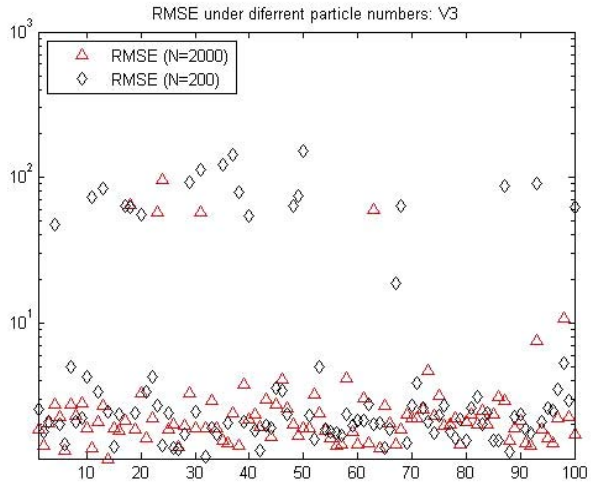

(b)

Figure 5.8 RMSE of PF-PDAF algorithm under different particles numbers for tracking scenarioV3 (Pd = 0.9, Cd = 0.5)

(a) RMSE_k value (averaged over 100 runs)

(b) RMSE^n value of 100 runs

5.5.3 Compare the Root Square PCRLB with RMSE of PF-PDAF Algorithm

This subsection compares the PCRLB, which is the theoretical achievable tracking accuracy, with the RMSE of the PF-PDAF algorithm. This comparison provides an indication of the tracking accuracy attained by the PF-PDAF algorithm under different settings of measurement origin uncertainty with varying clutter rates and detection rates. The PCRLB and the RMSE are obtained by averaging over 100 independent Monte Carlo runs. All simulations are based on the tracking scenario V3 (refer to Figure 5.1) with the

setting of SNR 37 dB, the mean $\mathbf{x}_{0|0}^{3}$ and covariance $\mathbf{P}_{0|0}^{3}$ of the prior target state estimate state and the particles number 1000.

Figure 5.9 shows the root square PCRLB under different detection rates with the clutter rate fixed for the tracking scenario V3. Figure 5.10 then compares the root square PCRLB with the RMSE_k value of the PF-PDAF algorithm under these settings. Figure 5.11 shows the root square PCRLB under different clutter rates with the detection rate fixed for the tracking scenario V3. Figure 5.12 then compares the root square PCRLB with the RMSE_k values of the PF-PDAF algorithm under these settings. Table 5.1 shows the root square PCRLB values which are averaged over 100 runs and the RMSE values which are averaged over all time steps and 100 runs under different detection rates with clutter rate fixed. Table 5.2 shows the root square PCRLB values which are averaged over 100 runs and the RMSE values which are averaged over all time steps and 100 runs under different clutter rates with detection rate fixed.

From the above figures and tables, we have the following findings: the RMSE of PF-PDAF algorithm is more affected by the lower detection rates or higher clutter rates than the PCRLB is; except at the very low level of measurement origin uncertainty, the RMSE of PF-PDAF is at least one order higher than root square PCRLB; and the sensitivity of PCRLB to the clutter and missed detections is not great. The significant gap between the PCRLB and the RMSE of PF-PDAF algorithm lies in the fact that the PCRLB is the bound on the performance of an optimal estimator while PF-PDAF algorithm is suboptimal. As proved in [50], for general tracking problems under measurement origin uncertainty, optimal estimation algorithms do not exist. However, the PCRLB shows the theoretically achievable (not necessarily attainable) tracking accuracy, and it could serve as a lower bound on the estimation error covariance of tracking algorithms. Therefore, in the next chapter, PCRLB will be used to act as the information utility measure in developing the sensing node selection scheme.

Throughout this chapter, we assumed that the detection rate P_d is a constant. In practical tracking applications, the detection rate will be a function that depends on the target-to-sensing node range, signal energy and noise energy. Such type detection rate may affect the performance of PF-PDAF algorithm. However, we will not give the detailed derivation of such type detection rate P_d in this thesis. Readers may refer to the related literature [27], [119].

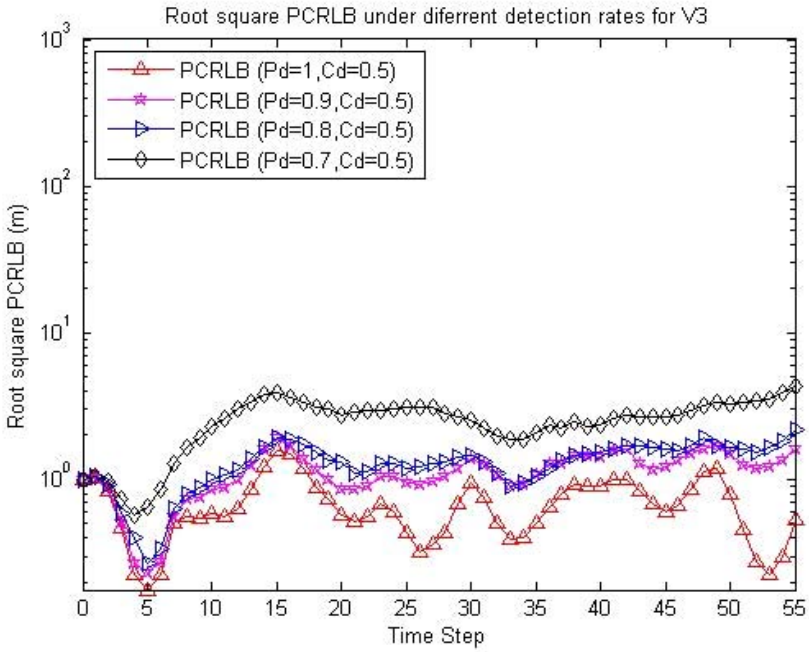

Figure 5.9 Root square PCRLB under different detection rates (Cd = 0.5) for tracking scenarioV3

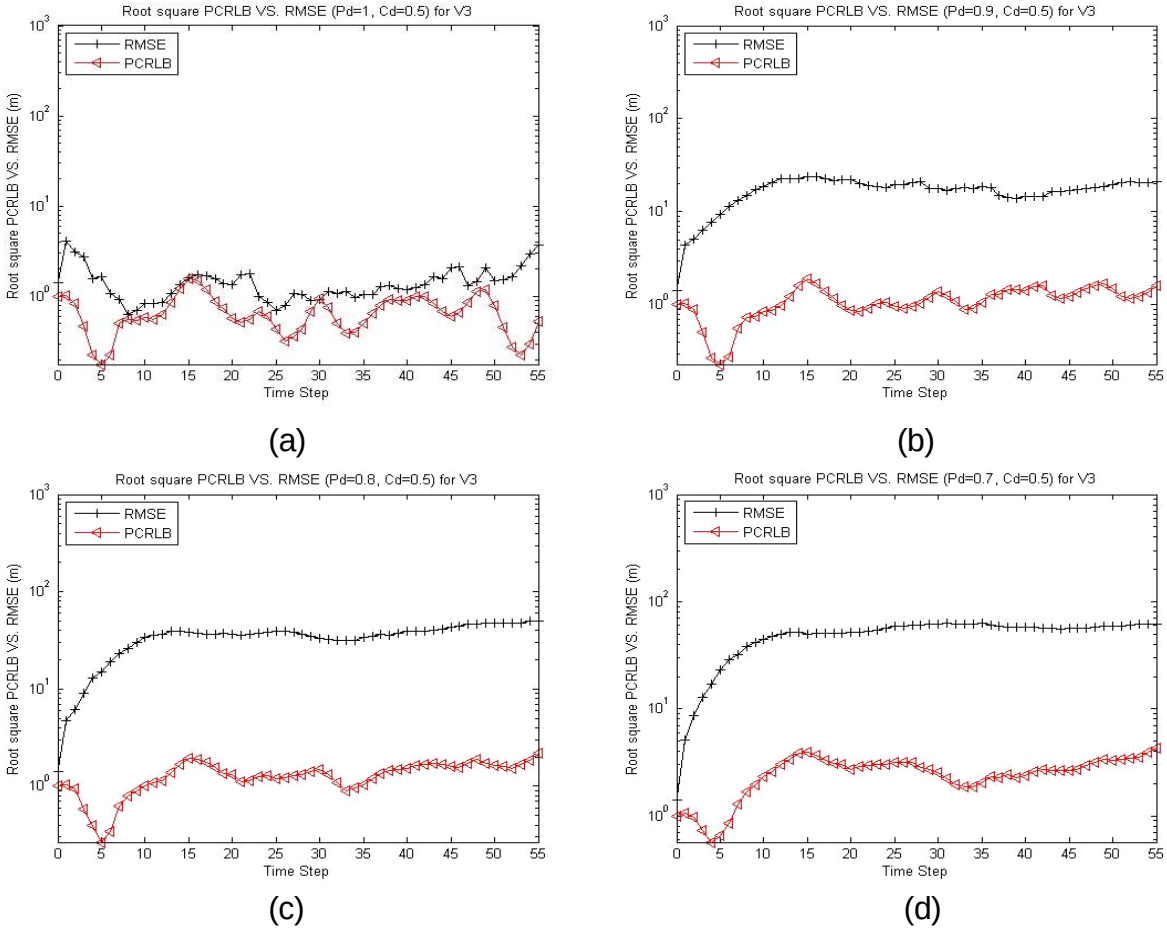

Figure 5.10 Root square PCRLB and $RMSE_k$ of PF-PDAF algorithm under different detection rates (Cd = 0.5) for tracking scenario V3 (averaged over 100 runs)
(a) Pd = 1 (b) Pd = 0.9 (c) Pd = 0.8 (d) Pd = 0.7

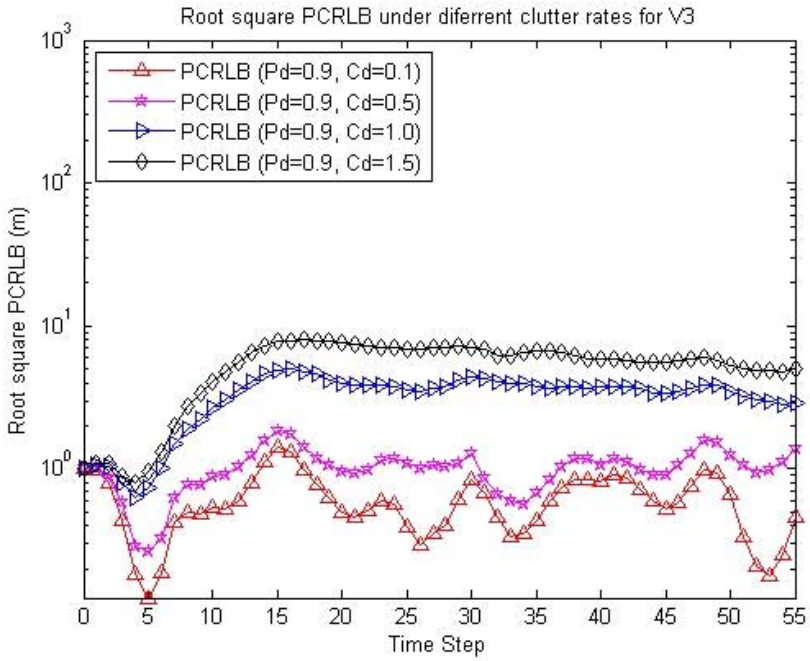

Figure 5.11 Root square PCRLB under different clutter rates (Pd = 0.9) for tracking scenarioV3

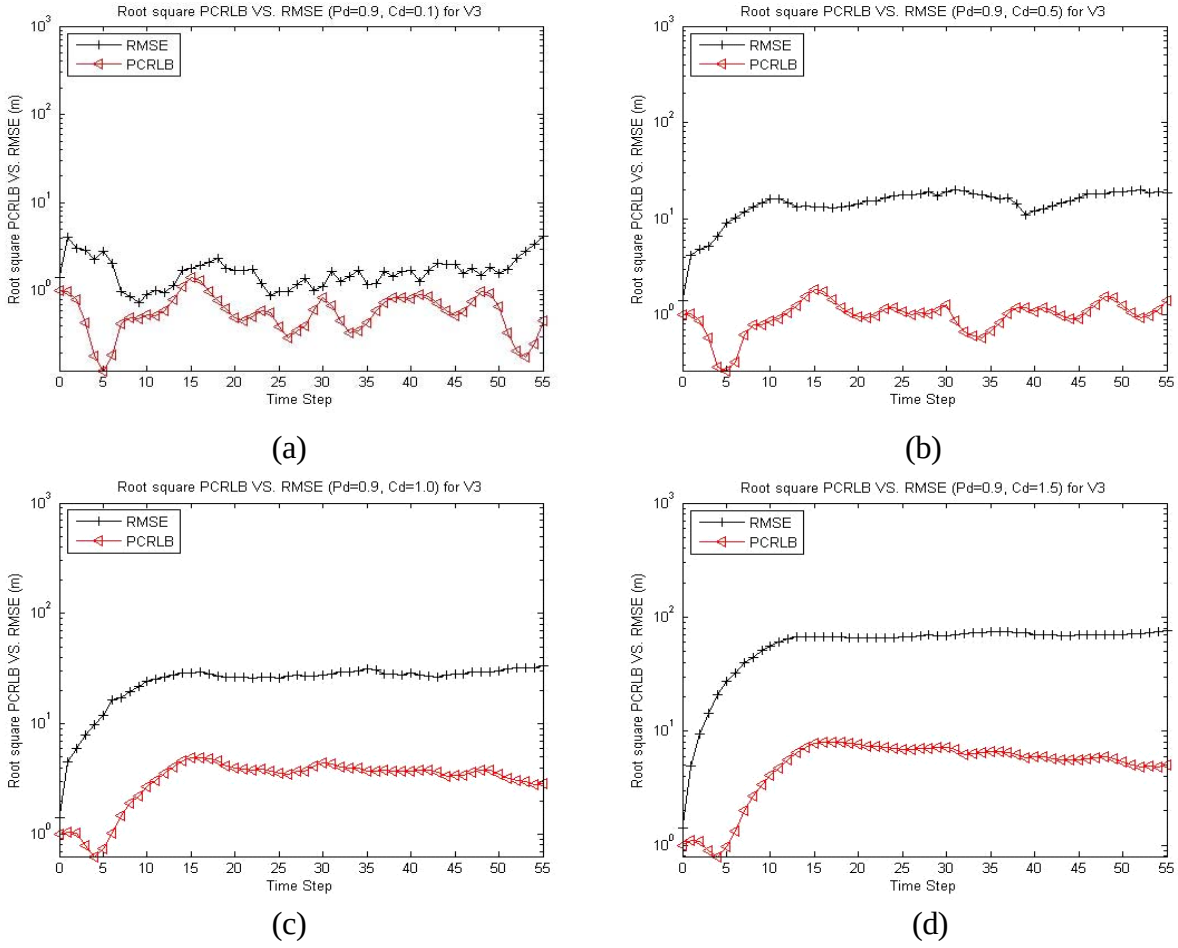

Figure 5.12 Root square PCRLB and RMSE_k of PF-PDAF algorithm under different clutter rates (Pd = 0.9) for tracking scenario V3 (averaged over 100 runs)
(a) Cd = 0.1 (b) Cd = 0.5 (c) Cd = 1.0 (d) Cd = 1.5

Table 5.1 Averaged $\sqrt{\text{PCRLB}}$ and RMSE at different detection rates (Cd=0.5)

Detection Rate	$\sqrt{\text{PCRLB}}$ (m)	RMSE (m)
Pd =1.0	0.6894	1.4779
Pd =0.9	1.1318	17.2641
Pd =0.8	1.3147	34.7461
Pd =0.7	2.5731	50.3521

Table 5.2 Averaged $\sqrt{\text{PCRLB}}$ and RMSE at different clutter rates (Pd=0.9)

Clutter Rate	$\sqrt{\text{PCRLB}}$ (m)	RMSE (m)
Cd =0.1	0.6161	1.7481
Cd =0.5	1.0239	14.8203
Cd =1.0	3.3194	25.4498
Cd =1.5	5.4865	61.1822

5.6 Summary

This chapter developed the PF-PDAF algorithm for tracking a single target under measurement origin uncertainty due to clutter and missed detections in wireless sensor networks. By adopting particles to represent the probability distribution function of the target state, the PF-PDAF algorithm could accommodate the general nonlinear state-space model while keeping the advantages of PDAF in effectively solving the data association problem. In order to provide a theoretical bound on the performance of PF-PDAF algorithm, the PCRLB under measurement origin uncertainty has also been derived and computed. It is shown that under measurement origin uncertainty, the measurement contribution to the PCRLB is a product of PCRLB when there is no measurement origin uncertainty and a scalar information reduction factor (IRF).

To minimize system resource utilisation in the wireless sensor networks, next chapter will develop distributive tracking algorithms including distributive PF, EKPF and PF-PDAF. Also by adopting particles representation of the probability density function of targets' states, Chapter 7 will develop algorithms for distributive tracking multiple targets under measurement origin uncertainty in wireless sensor networks.